Chapter 6

Heavy Quark Contribution to Longitudinal Structure Function F_L and the Ratio $R^h = \frac{F_L^h}{F_2^h}$ at Small-x

The dominant process for the heavy quark (charm and beauty quarks) production at HERA is the boson gluon fusion (BGF), where the photon interacts with a gluon from the proton by the exchange of a heavy quark pair and is given as $\gamma g \to q\bar{q}X$, with $q = c, b$ [1]. This reflects that the process is sensitive to the gluon density in the proton. Thus, the structure functions $F_k^h(k = 2, L; h = c, b)$ are dominated by the gluon content of the proton. The charm structure function F_2^c and the beauty structure function F_2^b are obtained from the measured charm and beauty cross sections after applying small corrections for the longitudinal structure functions F_L^c and F_L^b. At small values of x, F_L becomes non-negligible and its contribution should be properly taken into account while F_2 is extracted from the measured values of cross section. The same is also true for the contributions F_L^h to F_2^h due to the heavy quarks. In this chapter, the behaviour of heavy quark structure functions F_k^h with respect to Bjorken variable x are studied using Taylor expansion method and Regge behaviour of structure function at small-x. Here, we use the input distribution of gluon from Donnachie-Landshoff (DL) model [2] to determine the heavy flavour structure function of proton. The obtained results are compared with the recent HERA data [3, 4] and results of DL, Colour Dipole [5] models (CDM) and MSTW08 [6] parameterization which show good agreement with data and fit. We have used our results of heavy flavour structure function to analyze the behaviour of heavy

quark DIS cross section ratio $R^h(x,Q^2)$ and reduced cross section σ_r^h in heavy quark lepto-production at small values of x. We have also studied the behaviour of the heavy quark content of the F_L structure functions with respect to x.

6.1 Theory

6.1.1 Heavy quark contribution to F_L structure function using Taylor expansion method

In the small-x region, the heavy quark structure function is given by [7–9]

$$F_k^h(x,Q^2,m_h^2) = e_h^2 \frac{\alpha_s(\mu^2)}{\pi} \int_{ax}^1 \frac{dw}{w} C_{k,g}^h(w,\zeta) G\Big(\frac{x}{w},\mu^2\Big), \tag{6.1}$$

where $a = 1 + 4\zeta(\zeta = \dfrac{m_h^2}{Q^2})$, $m_h; (h = c,b)$ is the mass of the heavy quark and the renormalization scale μ is assumed to be either $\mu^2 = 4m_h^2$ or $\mu^2 = 4m_h^2 + Q^2$. $C_{k,g}^h; (k = 2, L)$ is the heavy quark co-efficient function which can be written up to NLO as [9]

$$C_{k,g}^h(w,\zeta) \rightarrow C_{k,g}^{(0)}(w,\zeta) + a_s(\mu^2)\Big[C_{k,g}^{(1)}(w,\zeta) + \overline{C}_{k,g}^{(1)}(w,\zeta) ln\frac{\mu^2}{m_h^2}\Big]. \tag{6.2}$$

Here $a_s(\mu^2) = \dfrac{\alpha_s(\mu^2)}{4\pi}$ and in NLO analysis

$$\alpha_s(\mu^2) = \frac{4\pi}{\beta_0 ln(\mu^2/\Lambda^2)} - \frac{4\pi\beta_1}{\beta_0^3} \frac{lnln(\mu^2/\Lambda^2)}{ln(\mu^2/\Lambda^2)}. \tag{6.3}$$

The co-efficient functions $C_{k,g}^{(0)}$ and $C_{k,g}^{(1)}$, $\overline{C}_{k,g}^{(1)}$ are at LO and NLO respectively. These have been computed up to NLO in ref. [7–10] and the expressions are given in Appendix B.

At small values of x we can rewrite the equation (6.1) by substituting $w = 1 - z$ as

$$F_k^h(x,Q^2) =< e^2 > \frac{\alpha_s(\mu^2)}{\pi} \int_0^{1-ax} \frac{dz}{1-z} C_{k,g}^h(1-z,\zeta) G\Big(\frac{x}{1-z},\mu^2\Big), \tag{6.4}$$

where F_k^h is derived from the integrated gluon distribution function $G(x,\mu^2)$. An approximate relationship between F_k^h and gluon distribution can be obtained from the expansion of $G\Big(\frac{x}{1-z},\mu^2\Big)$ around a particular choice of point of expansion. Since $ax < w < 1$, we have $0 < z < 1-ax$; so the series $\frac{x}{w} = \frac{x}{1-z}$ is convergent for $|z| < 1$. So, we can take the point of expansion z as any value between $0 \leq z < 1$.

Using the Taylor expansion method for the gluon distribution function at an arbitrary point $z = 0.8$ as described in chapter 4, and neglecting the higher order terms at small-x, $G\Big(\frac{x}{1-z},\mu^2\Big)$ can be written as

$$\begin{aligned} G\Big(\frac{x}{1-z},\mu^2\Big)\Big|_{z=0.8} &= G(z=0.8,\mu^2) + (z-0.8)\frac{\partial G(z=0.8,\mu^2)}{\partial x} \\ &= G(5x,\mu^2) + (z-0.8)\frac{\partial G(5x,\mu^2)}{\partial x}. \end{aligned} \tag{6.5}$$

Using equation (6.5) and leading order terms of equation (6.2) in equation (6.4) and performing the integration, we get

$$F_k^h(x,Q^2) = e_h^2\frac{\alpha_s(\mu^2)}{\pi}A(x)G\Big(5x+\frac{B(x)}{A(x)},\mu^2\Big) \tag{6.6}$$

where

$$A(x) = \int_0^{1-ax}\frac{dz}{1-z}[C_{k,g}^0(1-z)], \tag{6.7}$$

$$B(x) = \int_0^{1-ax}\frac{dz}{1-z}(z-0.8)[C_{k,g}^0(1-z)], \tag{6.8}$$

This result shows that the charm and beauty quark structure functions $F_k^h(x,Q^2)(k = 2, L; h = c, b)$ can be calculated using the low x gluon density from DL model [2] at LO. Similarly, we have also obtained the expression for the structure functions $F_k^h(x,Q^2)$ in NLO using the respective co-efficient function which is given by

$$F_k^h(x,Q^2) = e_h^2\frac{\alpha_s(\mu^2)}{\pi}P(x)G\Big(5x+\frac{Q(x)}{P(x)},\mu^2\Big), \tag{6.9}$$

$$P(x) = \int_0^{1-ax} \frac{dz}{1-z}\Big[C^0_{k,g}(1-z) + T_0\{C^1_{k,g}(1-z) + C^1_{k,g}(1-z)\}\Big] \tag{6.10}$$

and

$$Q(x) = \int_0^{1-ax} \frac{dz}{1-z}(z-0.8)\Big[C^0_{k,g}(1-z) + T_0(C^1_{k,g}(1-z) + C^1_{k,g}(1-z))\Big]. \tag{6.11}$$

Here, the numerical parameter T_0 is calculated from the data as described in chapter 2 and ref. [11]. Here $T_0 = 0.0278$ in our required Q^2 range $15 \leq Q^2 \leq 600GeV^2$.
Thus, we have calculated the charm and beauty quark structure functions F_L^c and F_2^c, F_L^b and F_2^b from the above equations (6.6) and (6.9)using the small-x gluon density from Donnachie Landshoff model [2].

The measurement of heavy quark structure function F_k^h are used to study the behaviour of DIS cross section ratio R^h which is related to the structure functions at small-x as

$$R^h = \frac{F_L^h}{F_2^h}. \tag{6.12}$$

Thus using the expressions for F_k^h, we get the LO and NLO relation for R^h as

$$R^h = \frac{A_L(x)}{A_2(x)} \tag{6.13}$$

and

$$R^h = \frac{P_L(x)}{P_2(x)}. \tag{6.14}$$

respectively.

The above expressions (6.13) and (6.14) show that the ratio is independent of the gluon distribution function and it depends only on the co-efficient function. Here, $A_L(x)$, $A_2(x)$, $P_L(x)$ and $P_2(x)$ are obtained by putting $k = L, 2$ in equations (6.7)and (6.10).

This ratio of structure function is useful to extract the heavy quark structure function from the reduced heavy quark cross section [3] at HERA. We have used this ratio R^h to determine the heavy quark reduced cross section at small-x.

Now the reduced cross section in terms of heavy quark structure function is given by

$$\begin{aligned}\sigma_r^h &= \frac{d^2\sigma^h}{dxdQ^2}\cdot\frac{xQ^4}{2\pi\alpha^2 Y_+} \\ &= F_2^h(x,Q^2,m_h^2) - \frac{y^2}{Y_+}F_L^h(x,Q^2,m_h^2) \\ &= F_2^h(x,Q^2,m_h^2)\Big(1-\frac{y^2}{Y_+}R^h\Big). \end{aligned} \tag{6.15}$$

Here $y=\frac{Q^2}{sx}$ is the inelasticity, with s the ep center-of-mass energy squared and $Y_+ = 1+(1-y)^2$. The above equation (6.15) relates the charm quark structure function to the reduced cross section via the ratio R^c. Thus, the behaviour of the ratio R^c and reduced cross section σ_r^c can be studied using the expressions (6.13), (6.14) and (6.15) with respect to the Bjorken variable x.

Again, the heavy quark content of the proton longitudinal structure function $K_L^h(x,Q^2,m_h^2)$ at small-x is determined using the relation [12]

$$K_L^h(x,Q^2,m_h^2) = \frac{F_L^h(x,Q^2,m_h^2)}{F_L^h(x,Q^2,m_h^2)+F_L^g(x,Q^2)}. \tag{6.16}$$

Here we have used the results of F_L^g from chapter 4 to calculate the quantity K_L^h.

6.1.2 Heavy quark contribution to F_L structure function using Regge approach

In the small-x region, the heavy quark structure function is given by [7–9]

$$F_k^h(x,Q^2,m_h^2) = e_h^2\frac{\alpha_s(\mu^2)}{\pi}\int_{ax}^1\frac{dw}{w}C_{k,g}^h(w,\zeta)G\Big(\frac{x}{w},\mu^2\Big), \tag{6.17}$$

where a, $m_h; (h = c, b)$, μ and $C^h_{k,g}; (k = 2, L)$ are mentioned in the previous subsection i.e., (6.1.1).

Now, the Regge like behaviour of the gluon distribution function can be expressed as [13]

$$G(x, \mu^2) = f(\mu^2) x^{-\lambda_g}, \tag{6.18}$$

where $f(\mu^2)$ is a function of μ^2 and λ_g is the Regge exponent. Now, $G\Big(\frac{x}{w}, \mu^2\Big)$ can be written as

$$G\Big(\frac{x}{w}, \mu^2\Big) = G(x, \mu^2) w^{\lambda_g}. \tag{6.19}$$

Using equations (6.18) and (6.19) in equation (6.17) we get

$$F^h_k(x, Q^2, m^2_h) = e^2_h \frac{\alpha_s(\mu^2)}{\pi} \int_{ax}^1 \frac{dw}{w} C^h_{k,g}(w, \zeta) w^{\lambda_g} G(x, \mu^2). \tag{6.20}$$

Using the above equation we have calculated the charm and beauty quark structure function in LO and NLO using the respective co-efficient functions and the low x gluon density from DL model [2]. We have also calculated the heavy quark DIS cross section ratio R^h and reduced cross section σ^h_r using the expressions (6.12) and (6.15) with the help of the results of F^h_k obtained from the equation (6.20). Lastly, to evaluate the quantities K^c_L and K^b_L using relation (6.16), we have used the results of F^g_L from chapter 5.

6.2 Results and Discussions

In this chapter, we have determined the charm and beauty quark structure functions $F^h_k(k = 2, L; h = c, b)$, ratio of heavy quark structure function R^h and reduced cross section σ^h_r in NLO approximation using Taylor expansion method and Regge like behaviour of structure function. Here we have compared our calculated results with

recent experimental H1, ZEUS data, results of DL, CD model, MSTW08 parameterization and results obtained by other author. Inclusive charm and beauty cross sections are measured in e^-p and e^+p neutral current collisions at HERA in the kinematic range $2 \times 10^{-4} \leq x \leq 0.05$ and $5 \leq Q^2 \leq 2000 GeV^2$. In our analysis, we have studied the behaviour of our results in the range $10^{-4} \leq x \leq 0.1$ and $20 \leq Q^2 \leq 600 GeV^2$.

6.2.1 Charm quark contribution to structure functions

(A)Results using Taylor expansion method

The charm structure functions F_L^c and F_2^c have been determined from the expressions (6.6) and (6.9) using the respective charm quark co-efficient functions in LO, NLO and the gluon distribution function of DL model. Here the gluon distribution function is expanded at $z = 0.8$ using the Taylor expansion method.

Figures 6.1 and 6.2 describe the behaviour of F_L^c and F_2^c structure functions with respect to x. Here the results of F_2^c structure functions are compared with recent H1 and ZEUS data. Both the charm quark components of the structure function increase towards small values of x for fixed Q^2 values. To confirm the behaviour of these structure functions we have also calculated the ratio of charm quark structure function R^c and the charm quark reduced cross section σ_r^c using the relations (6.13), (6.14) and (6.15). Figure 6.3 shows the behaviour of the predicted ratio R^c as a function of x for fixed values of Q^2. It is observed that this ratio is almost independent of x at small values of x irrespective of Q^2 values. The plots in figure 6.4 show the results of reduced cross section σ_r^c in comparison with H1 [3] and ZEUS [4] data. We have also compared our results of charm quark component of structure functions F_L^c and F_2^c with the DL, colour dipole model (CDM) [5] and results obtained by Boroun et al (GRB) [14] which are depicted in figures 6.5 and 6.6. In color dipole model the excitation of heavy flavors in DIS at small-x is described in terms of interaction of small size quark-antiquark color dipoles in the photon [5]. In a recent paper [14], Boroun et al have reported

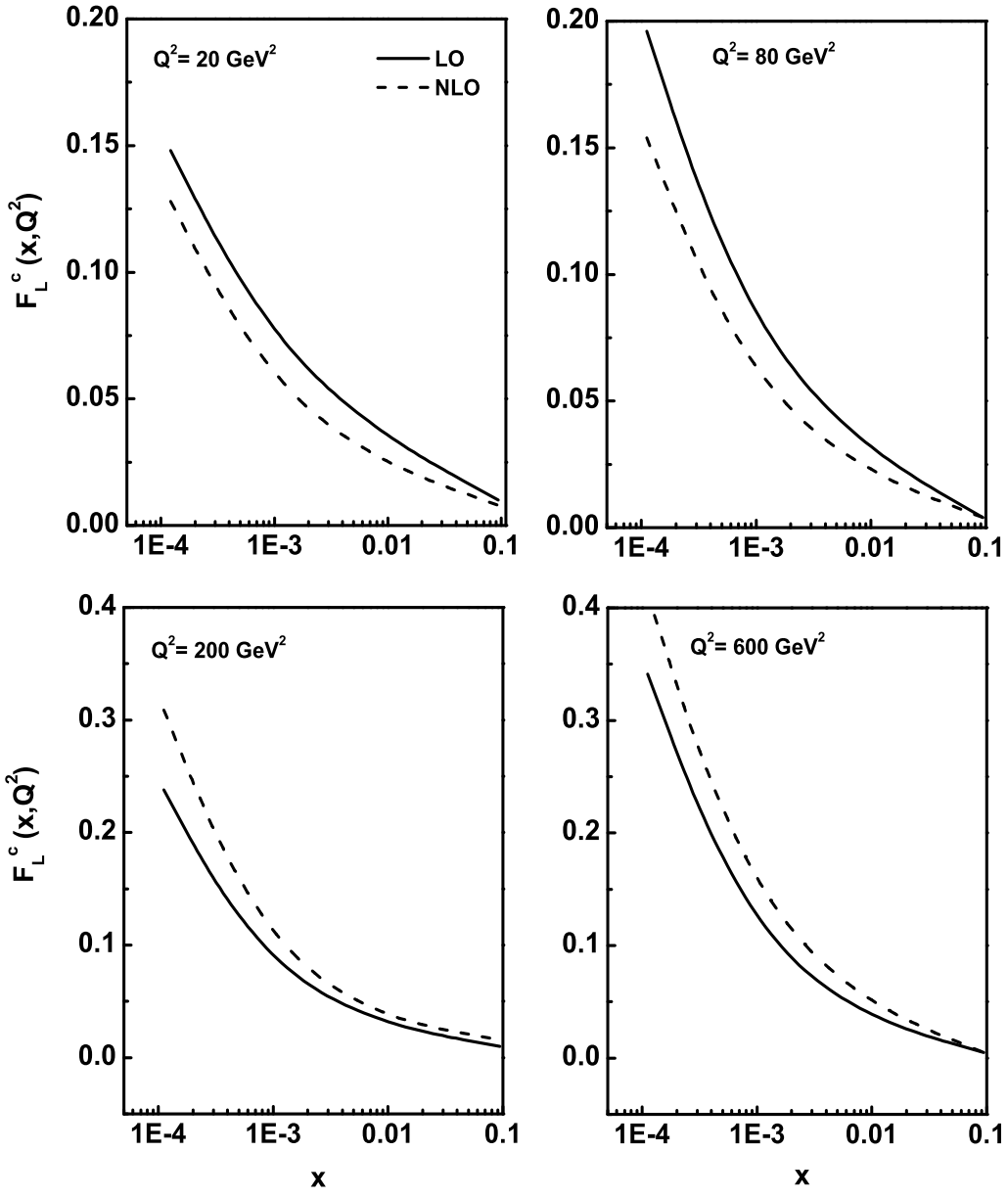

Figure 6.1: x-evolution results of F_L^c structure function using Taylor expansion method with the input gluon distribution from DL model.

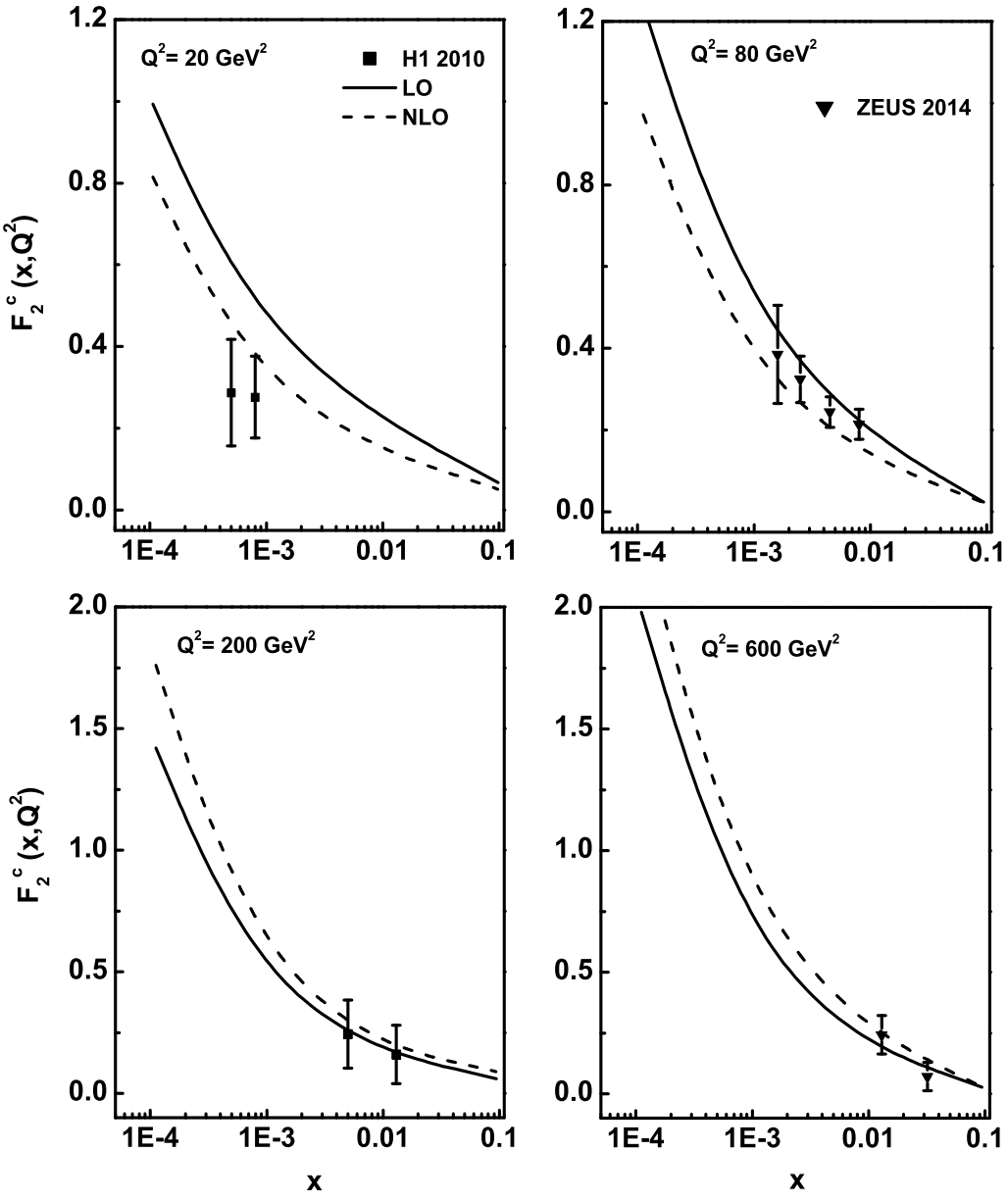

Figure 6.2: x-evolution results of F_2^c structure function using Taylor expansion method in comparison with the H1, ZEUS data.

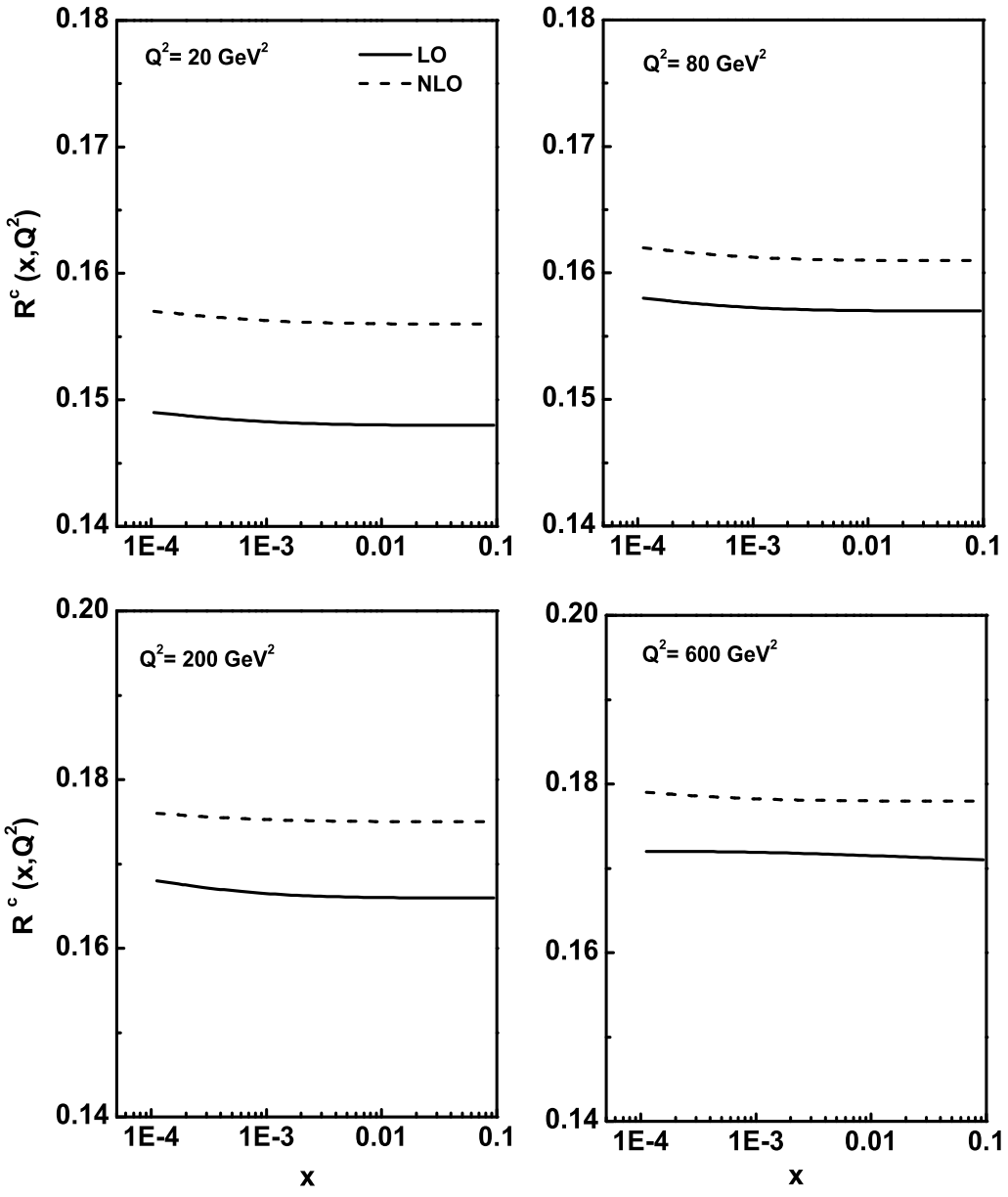

Figure 6.3: x-evolution results of the ratio of the charm quark structure functions R^c using Taylor expansion method.

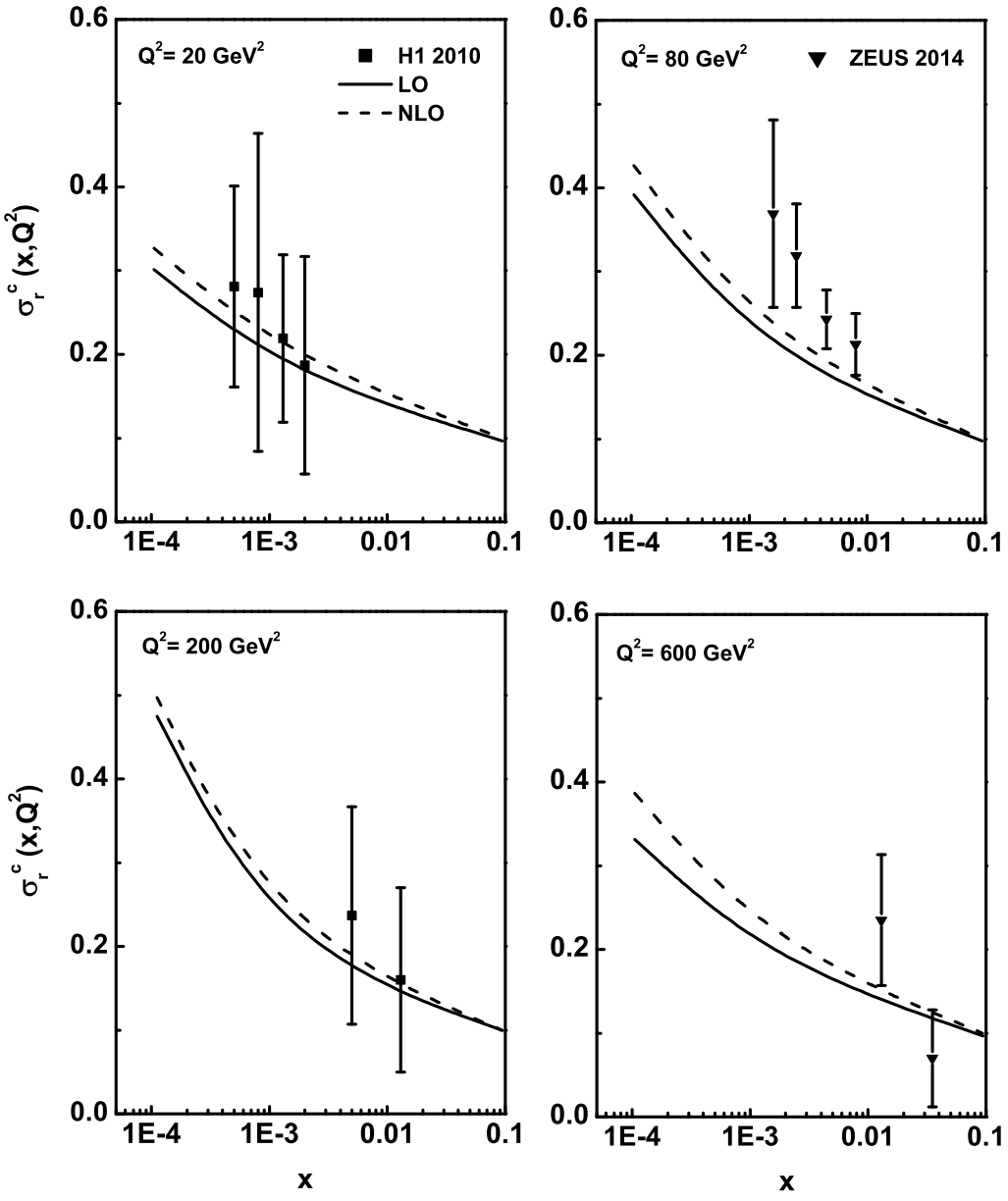

Figure 6.4: x-evolution results of charm quark reduced cross section σ_r^c using Taylor expansion method in comparison with the H1, ZEUS data.

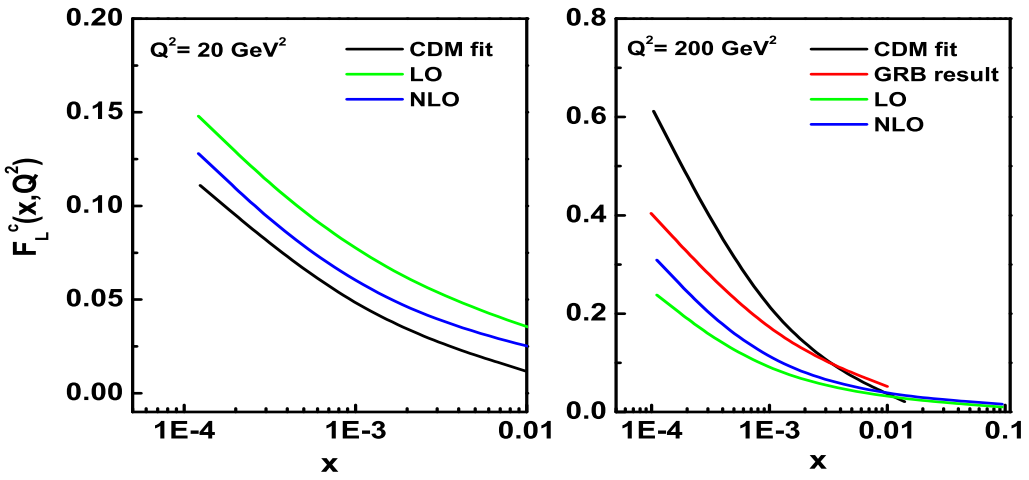

Figure 6.5: Comparison of our results of F_L^c at $Q^2 = 20, 200GeV^2$ using Taylor expansion method with the results of colour dipole model (CDM) and Boroun et al (GRB).

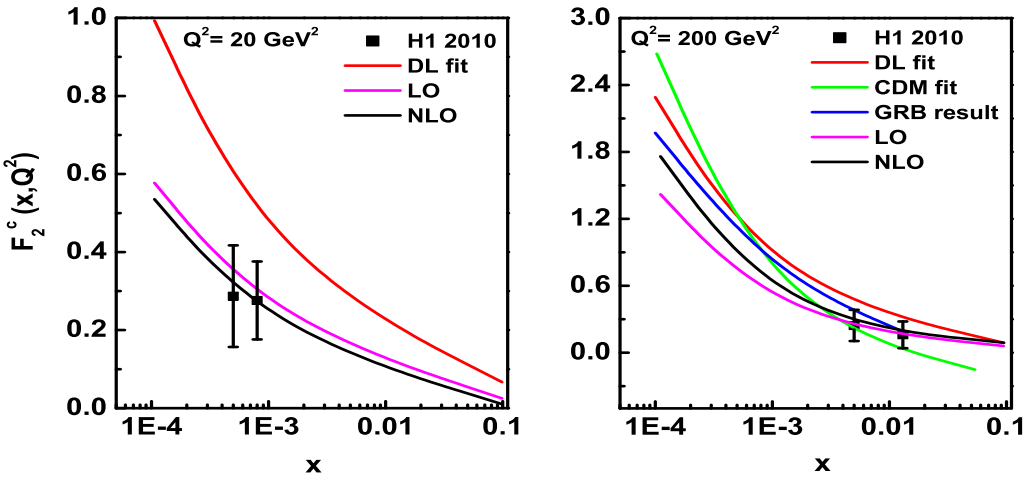

Figure 6.6: Comparison of our results of F_2^c at $Q^2 = 20, 200GeV^2$ using Taylor expansion method with the results of DL, colour dipole model (CDM) and Boroun et al (GRB).

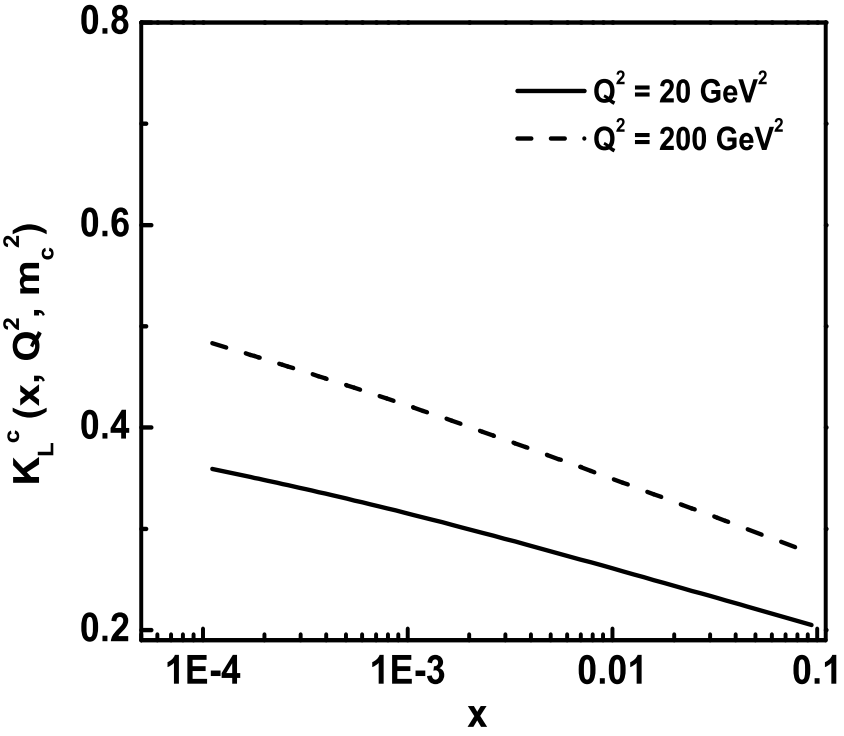

Figure 6.7: Results of the charm content of F_L structure function K_L^c with respect to x at $Q^2 = 20, 200 GeV^2$ using Taylor expansion method.

that the charm quark structure function F_k^c have a hard pomeron behaviour at low x which shows good agreement with data. In all the cases in our calculations we take the value of $m_c = 1.2GeV$ and renormalization scale μ as $\mu^2 = 4m_c^2 + Q^2$. We observed that our results for charm quark structure functions show good agreement with the data at this renormalization scale. Finally we present the charm content of the proton longitudinal structure function $K_L^c(x, Q^2, m_c^2)$ at small-x in figure 6.7. It is observed from the figure that charm content of the structure function grows towards small-x and increasing values of Q^2.

(B) Results using Regge behaviour of structure function

The charm quark structure functions F_L^c and F_2^c have been determined from the expression (6.20) using the respective charm quark co-efficient function in LO, NLO and the results of gluon distribution function obtained using the Regge behaviour of structure function in chapter 5. Here the input distribution of gluon is taken from the DL model. Figures 6.8 and 6.9 describe the behaviour of F_L^c and F_2^c structure function with respect to x. Here the results of F_2^c structure function are compared with recent H1 and ZEUS data. In both the cases, charm quark components of the structure function increases towards small values of x for fixed Q^2 values. To confirm the behaviour of these structure functions we have also calculated the ratio of charm quark structure function R^c and the charm quark reduced cross section σ_r^c using the relations (6.12) and (6.15). The behaviour of the predicted ratio R^c as a function of x for fixed values of Q^2 is depicted in figure 6.10. It is observed that this ratio is independent of x at small values of x irrespective of Q^2 values. The plots in figure 6.11 shows the results of reduced cross section σ_r^c in comparison with H1 [3] and ZEUS [4] data.

We have also compared our results of charm quark component of structure functions F_L^c and F_2^c with the DL, colour dipole model (CDM) [5] and results obtained by Boroun et al (GRB) which are depicted in figures 6.12 and 6.13. In color dipole model (CDM) the excitation of heavy flavors in DIS at small-x is described in terms of interaction of small size quark-antiquark color dipoles in the photon [5]. In all the cases in our calculations using Regge behaviour of structure function, we take the value of $m_c = 1.2GeV$ and renormalization scale μ as $\mu^2 = 4m_c^2 + Q^2$. We observed that our results for charm quark structure functions show good agreement with the data at this renormalization scale. We have also presented the charm content of the proton longitudinal structure function $K_L^c(x, Q^2, m_c^2)$ at small-x in figure 6.14. It is observed from the figure that charm content of the structure function grows towards small-x and increasing values of Q^2.

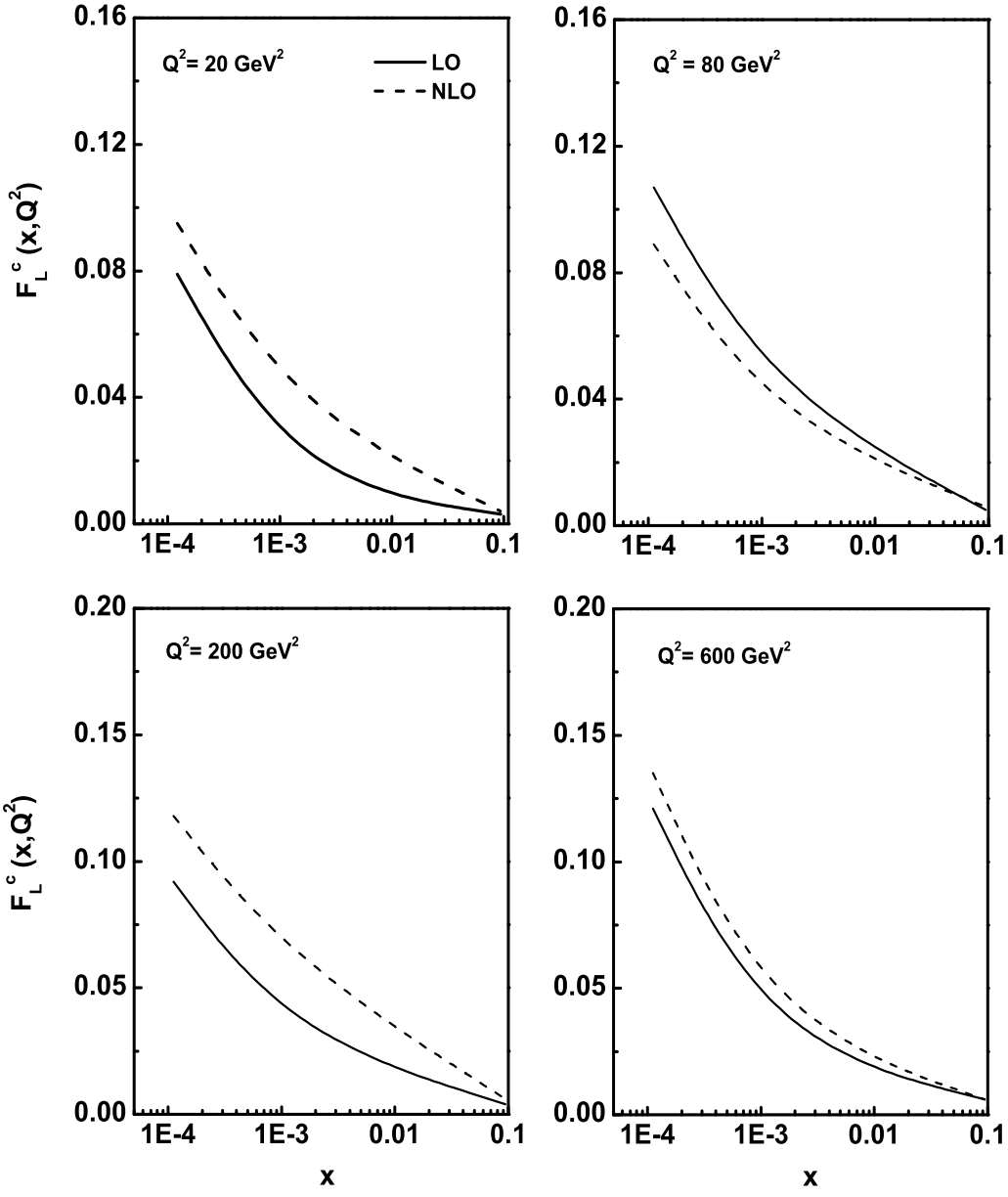

Figure 6.8: x-evolution results of F_L^c structure function using Regge theory with the input gluon distribution from DL model.

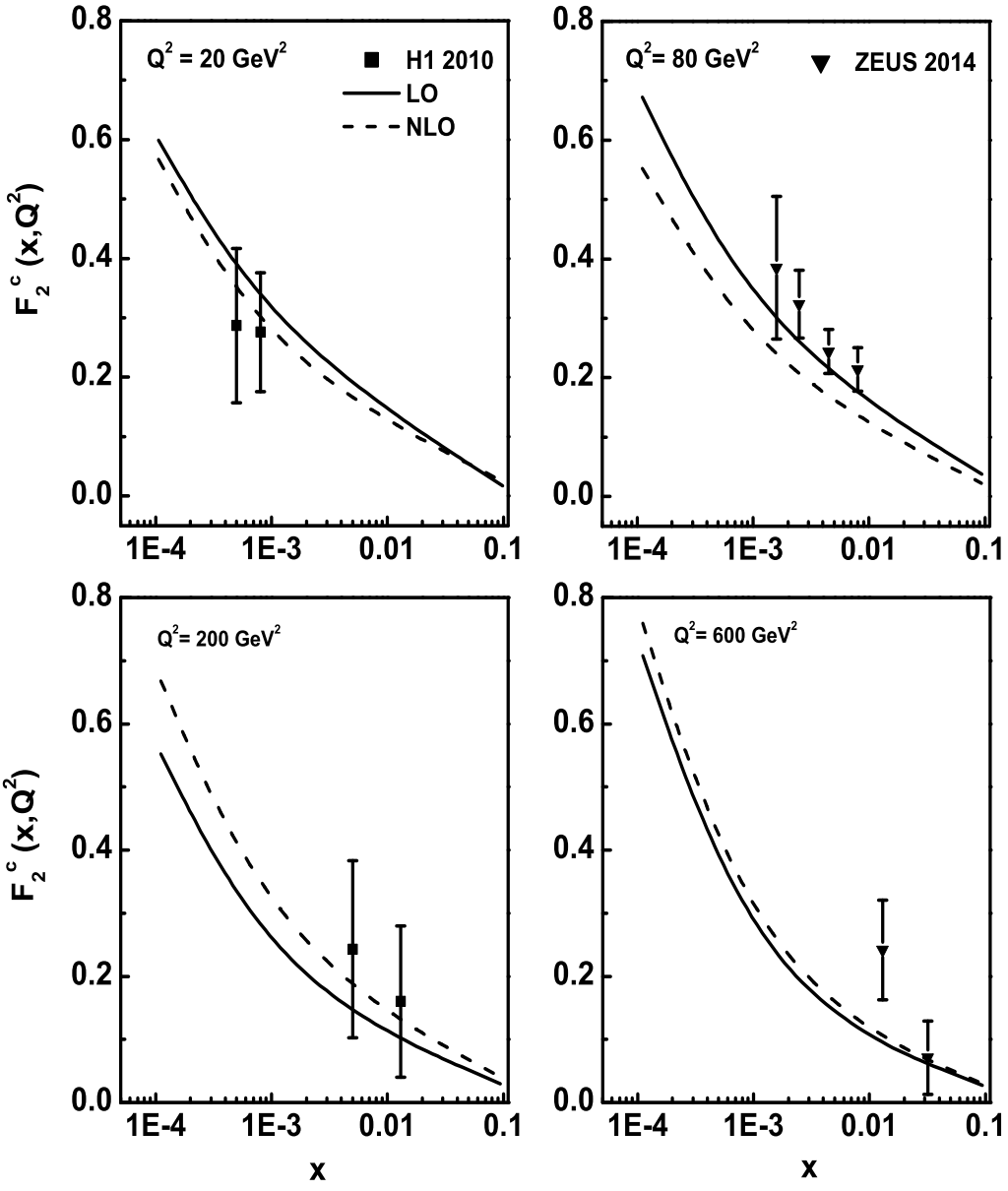

Figure 6.9: x-evolution results of F_2^c structure function using Regge theory in comparison with the H1, ZEUS data.

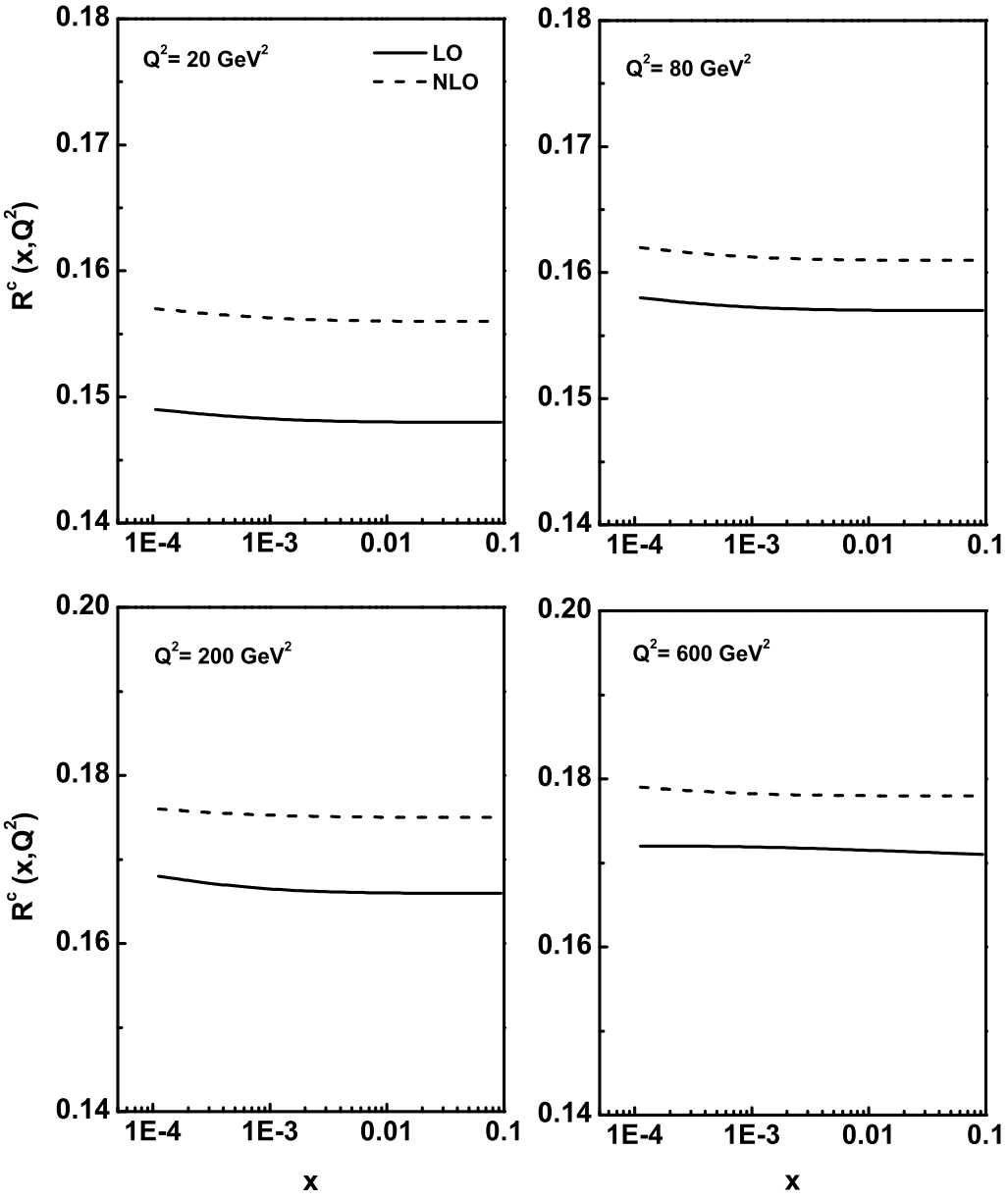

Figure 6.10: x-evolution results of the ratio of the charm quark structure function R^c using Regge theory.

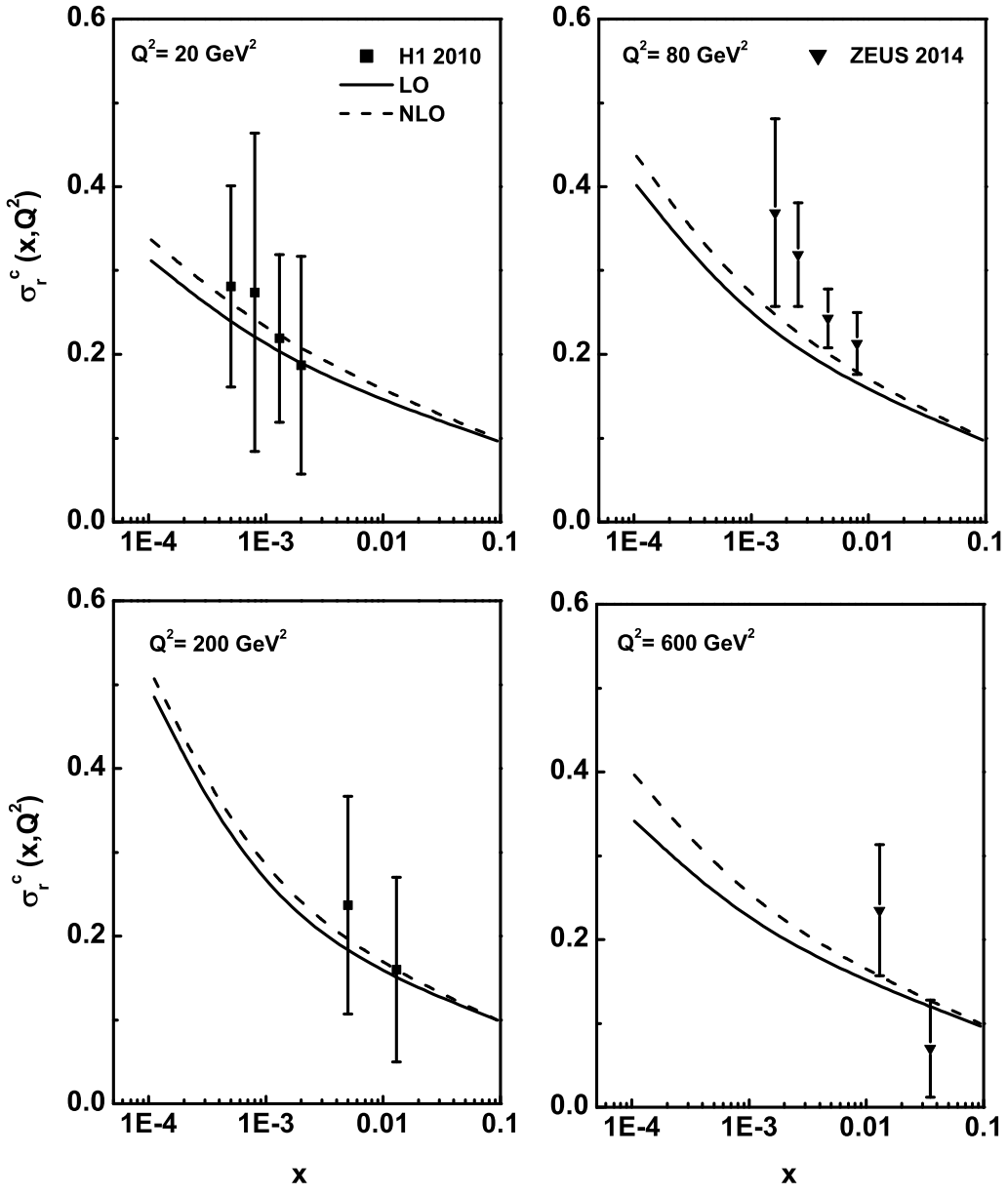

Figure 6.11: x-evolution results of the charm quark reduced cross section σ_r^c using Regge theory in comparison with the H1, ZEUS data.

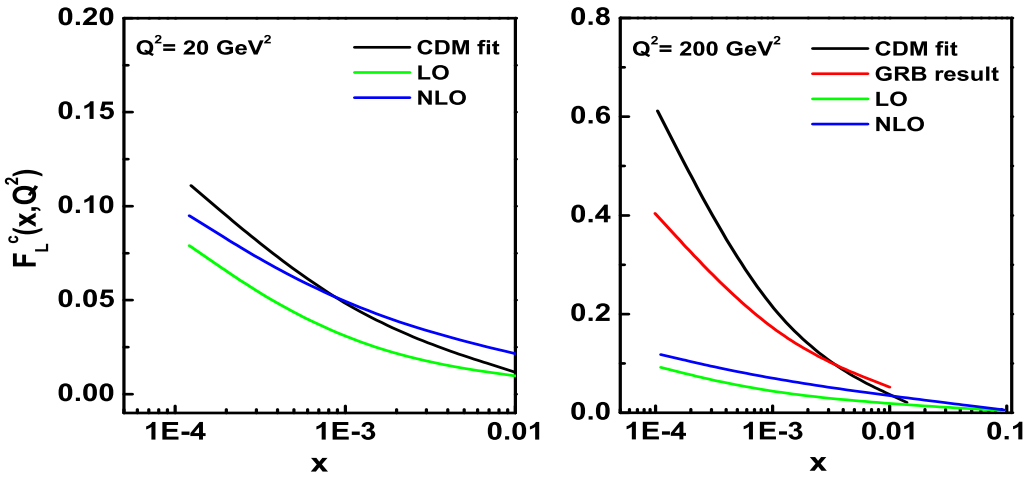

Figure 6.12: Comparison of our results of F_L^c at $Q^2 = 20, 200 GeV^2$ using Regge theory with the results of CD model and Boroun et al (GRB).

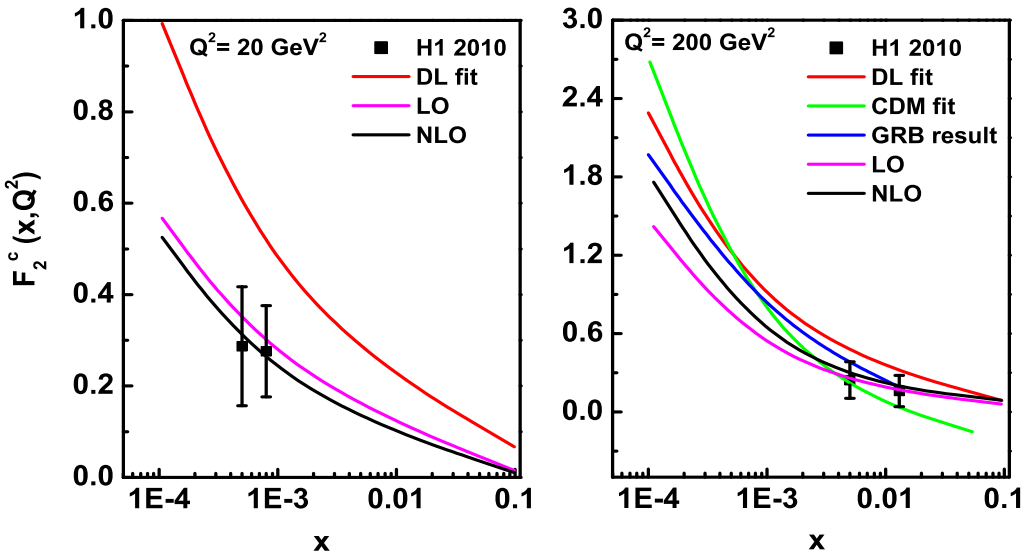

Figure 6.13: Comparison of our results of F_2^c at $Q^2 = 20, 200 GeV^2$ using Regge theory with the results of DL, CD model and Boroun et al (GRB).

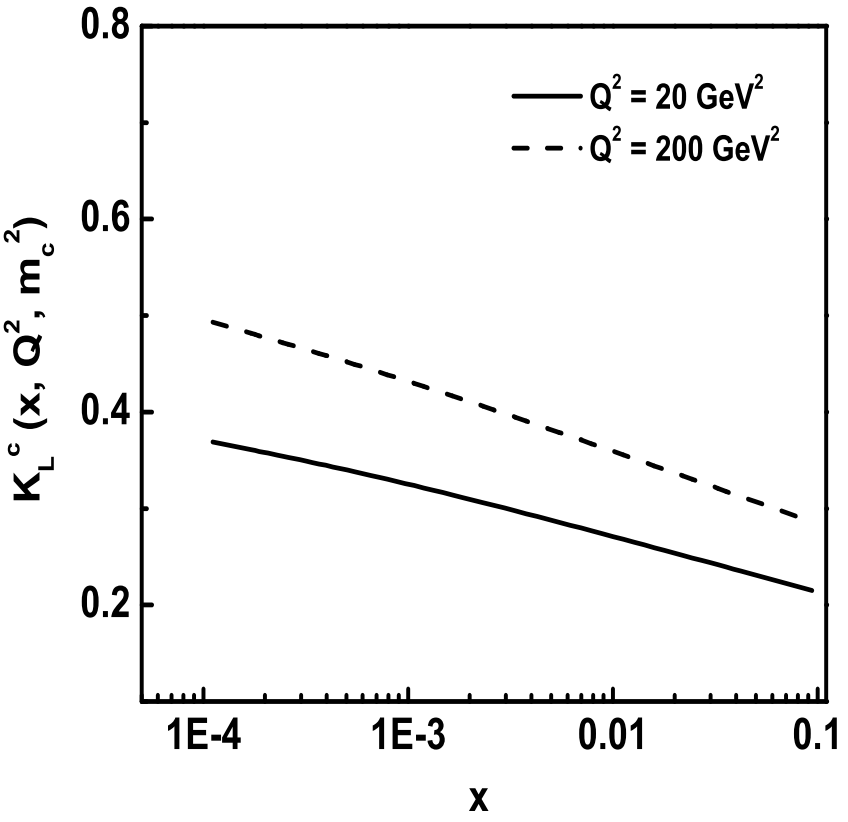

Figure 6.14: Results of the charm content of F_L structure function K_L^c with respect to x at $Q^2 = 20, 200 GeV^2$ using Regge theory.

6.2.2 Beauty quark contribution to structure functions

(A)Results using Taylor expansion method

The beauty quark structure functions F_L^b and F_2^b have been determined from the expressions (6.6) and (6.9) using the respective beauty quark co-efficient functions in LO, NLO and the gluon distribution function of DL model. Here the gluon distribution function is expanded at $z = 0.8$ using the Taylor expansion method. Figures 6.15 and 6.16 describe the behaviour of F_L^b and F_2^b structure functions with respect to x. Here

the results of F_2^b structure function are compared with recent H1 and ZEUS data. Both the beauty quark components of the structure function increase towards small values of x for fixed Q^2 values. To confirm the behaviour of these structure functions we have also calculated the ratio of beauty quark structure function R^b and the beauty quark reduced cross section σ_r^b using the relations (6.13), (6.14) and (6.15). Figure 6.17 shows the behaviour of the predicted ratio R^b as a function of x for fixed values of Q^2. It is observed that this ratio is independent of x at small values of x irrespective of Q^2 values. The plots in Figure 6.18 shows the results of reduced cross section σ_r^b in comparison with H1 [3] and ZEUS [4] data. In these plots also our results show good agreement with the experimental data.

We have also compared our results of beauty quark component of structure functions F_2^b with the results of MSTW08 parameterization which are depicted in figure 6.19. In all the cases in our calculations we take the value of $m_b = 4.2GeV$ and renormalization scale μ as $\mu^2 = 4m_b^2 + Q^2$. We observed that our results for beauty quark structure function show good agreement with the data at this renormalization scale. Finally we present the beauty content of the proton longitudinal structure function $K_L^b(x, Q^2, m_b^2)$ at small-x in figure 6.20. It is observed from the figure that beauty content of the structure function grows towards small-x and increasing values of Q^2.

(B) Results using Regge behaviour of structure function

The beauty quark structure functions F_L^b and F_2^b have been determined from the expression (6.20) using the respective beauty quark co-efficient functions in LO, NLO and the results of gluon distribution function obtained using the Regge behaviour of structure function in chapter 5. Here the input distribution of gluon is taken from the DL model. Figures 6.21 and 6.22 describe the behaviour of F_L^b and F_2^b structure function with respect to x. Here the results of F_2^b structure function are compared with recent H1 and ZEUS data. In both the cases, beauty quark components of the

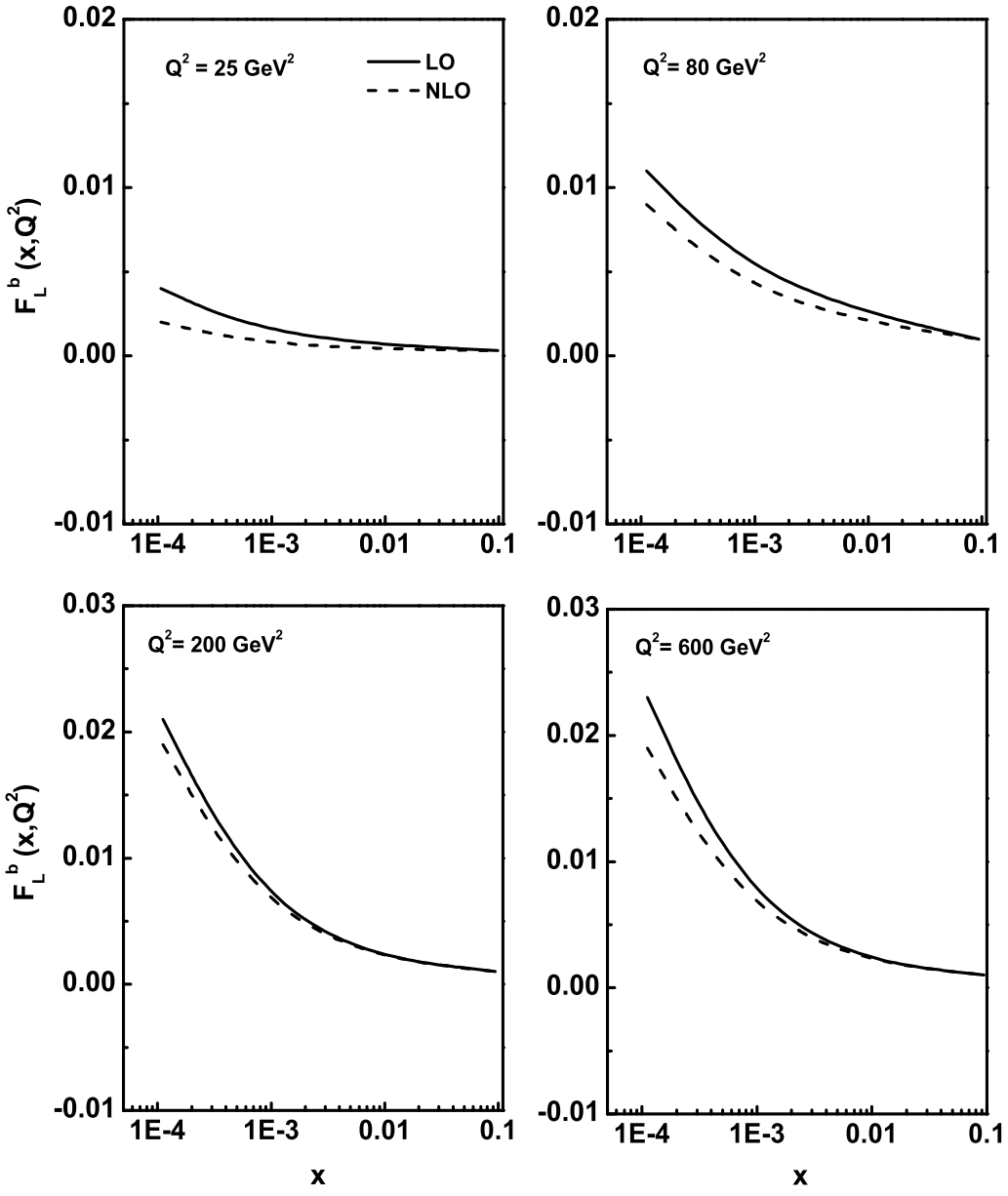

Figure 6.15: x-evolution results of F_L^b structure function using Taylor expansion method with the input gluon distribution from DL model.

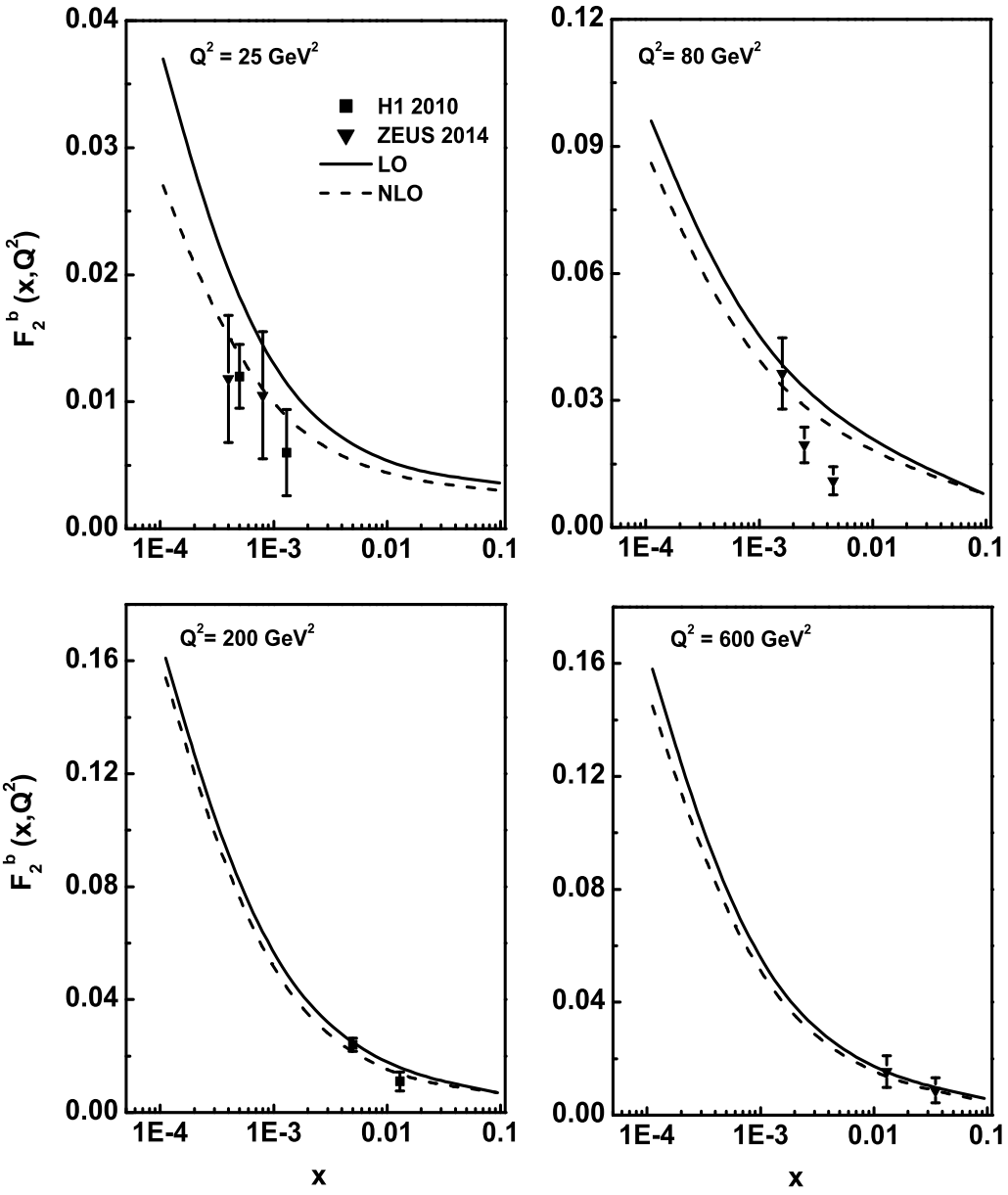

Figure 6.16: x-evolution results of F_2^b structure function using Taylor expansion method in comparison with the H1, ZEUS data.

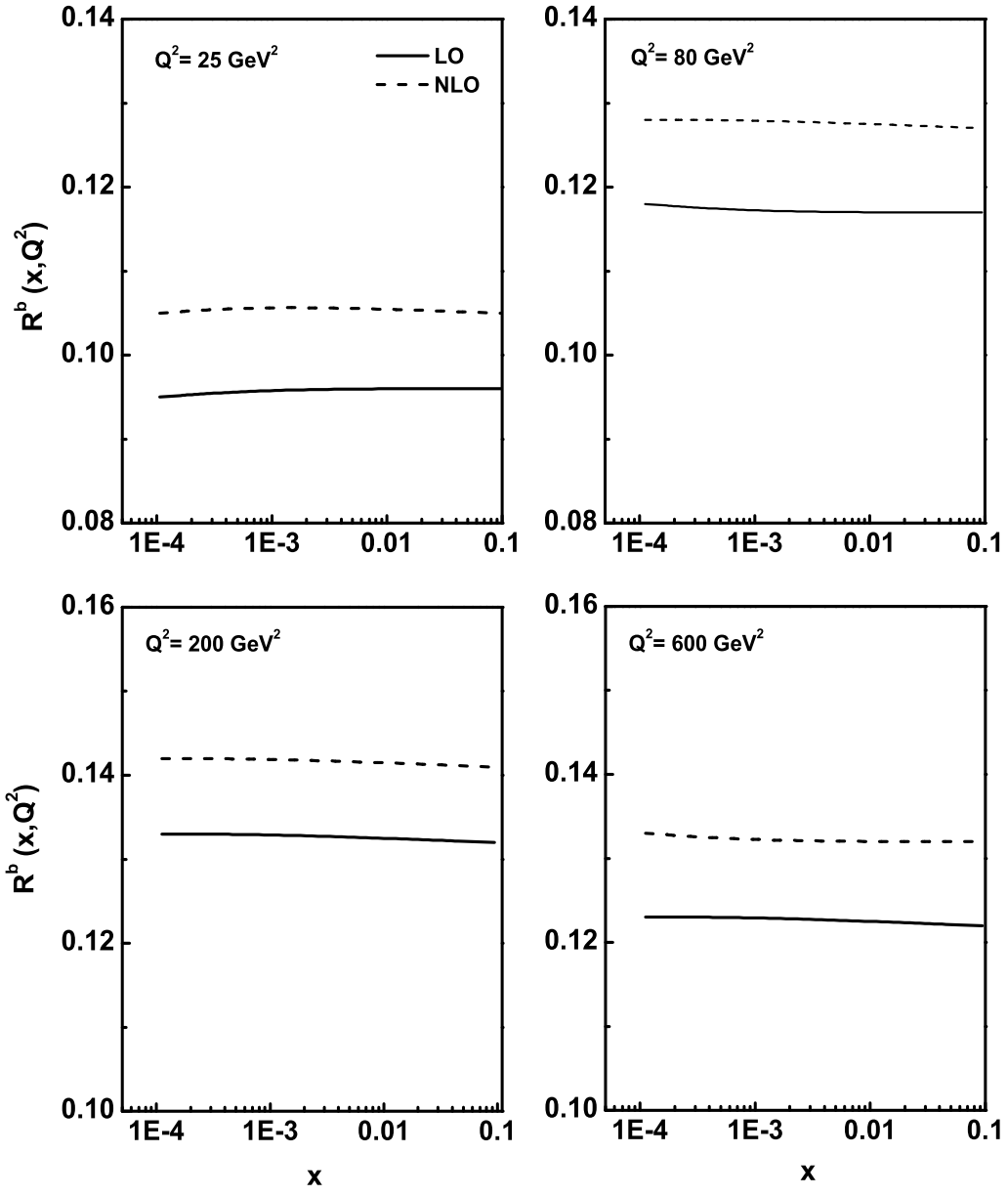

Figure 6.17: x-evolution results of the ratio of the beauty quark structure functions R^b using Taylor expansion method .

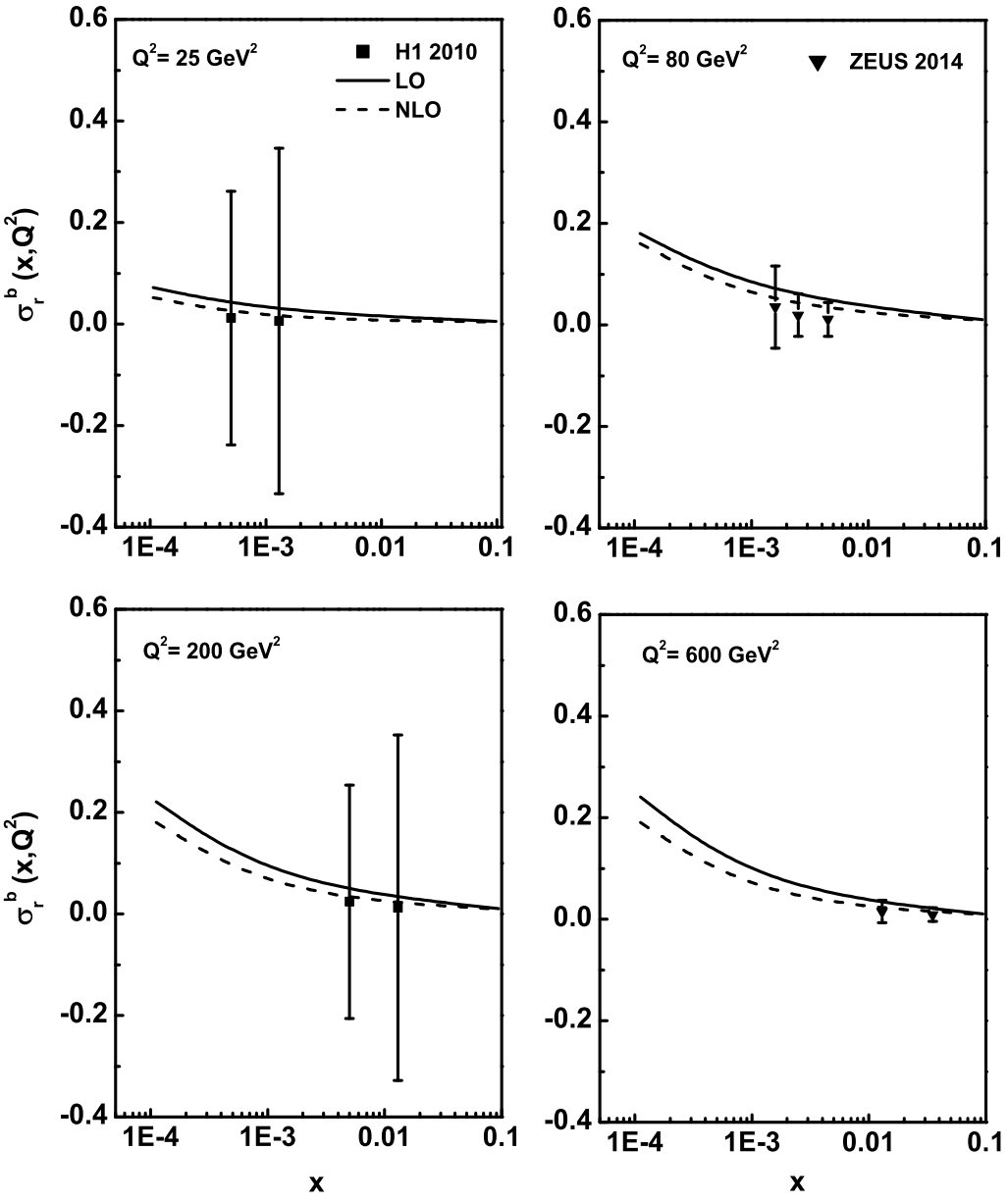

Figure 6.18: x-evolution results of the beauty quark reduced cross section σ_r^b using Taylor expansion method in comparison with the H1, ZEUS data.

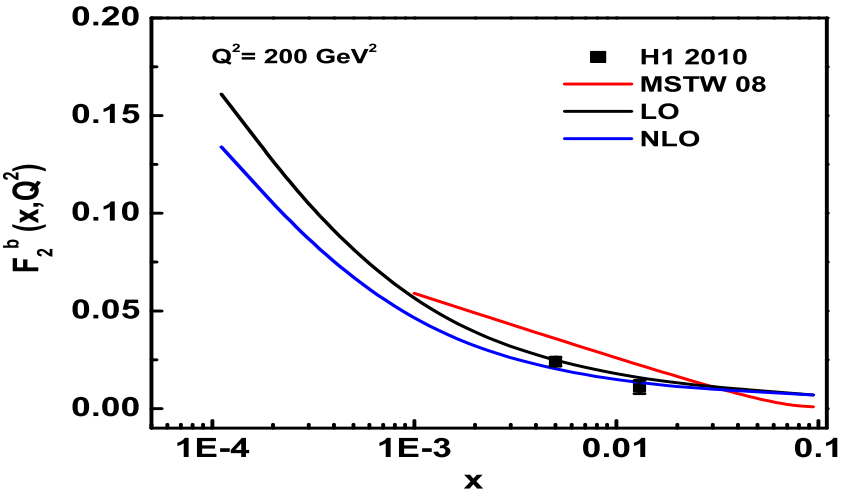

Figure 6.19: Comparison of our results of F_2^b at $Q^2 = 200GeV^2$ using Taylor expansion method with the results of MSTW 08.

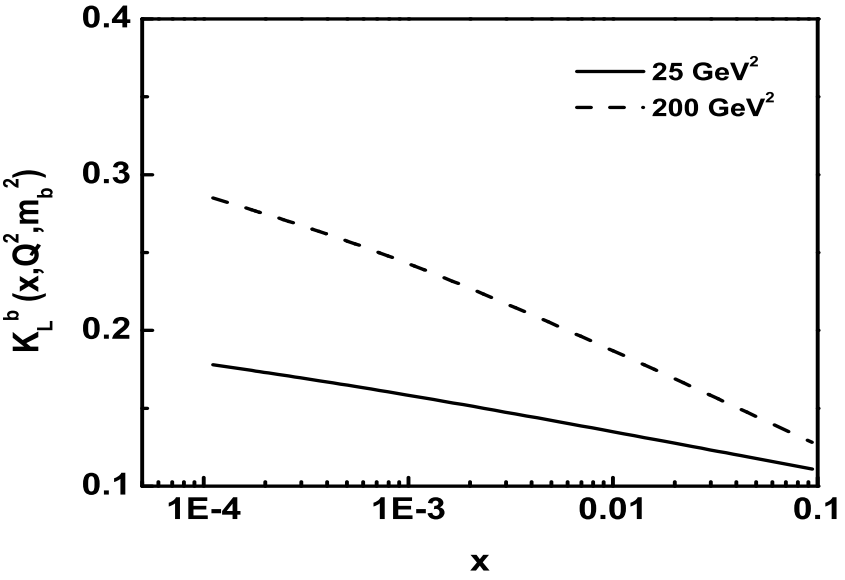

Figure 6.20: Results of the beauty content of F_L structure function K_L^b with respect to x at $Q^2 = 25, 200GeV^2$ using Taylor expansion method.

structure function increase towards small values of x for fixed Q^2 values. To confirm the behaviour of these structure functions we have also calculated the ratio of beauty quark structure function R^b and the beauty quark reduced cross section σ_r^b using the relations (6.12) and (6.15) respectively. The behaviour of the predicted ratio R^b as a function of x for fixed values of Q^2 is depicted in figure 6.23. It is observed that this ratio is independent of x at small values of x irrespective of Q^2 values. The plots in figure 6.24 show the results of reduced cross section σ_r^b in comparison with H1 [3] and ZEUS [4] data.

We have also compared our results of beauty quark structure functions F_2^b with the results of MSTW08 parameterization which are depicted in figure 6.25. We have also presented the beauty content of the proton longitudinal structure function $K_L^b(x, Q^2, m_b^2)$ at small-x in figure 6.26. It is observed from the figure that beauty content of the structure function grows towards small-x and increasing values of Q^2.

(C) Comparative study of the results of the heavy quark reduced cross section obtained by both the methods

The results of heavy quark structure functions, their ratio and the reduced cross section obtained by both the methods i.e., Taylor expansion method and Regge theory show good agreement with the available experimental data, model fit and parameterization. The heavy quark reduced cross section is calculated using the heavy quark structure function and their ratio. The behaviours of ratio of heavy quark structure functions in both the cases are same as these are independent of the distribution of gluons inside proton. Here we have presented the comparative analysis of the behaviours of charm and beauty quark reduced cross sections σ_r^c and σ_r^b with respect to x for different values of Q^2 obtained by both the methods which are depicted in figures 6.27 and 6.28. Both the figures show that our results are in good agreement with the experimental results. Figure 6.29 shows the sensitivity of our results of σ_r^c and σ_r^b with the mass

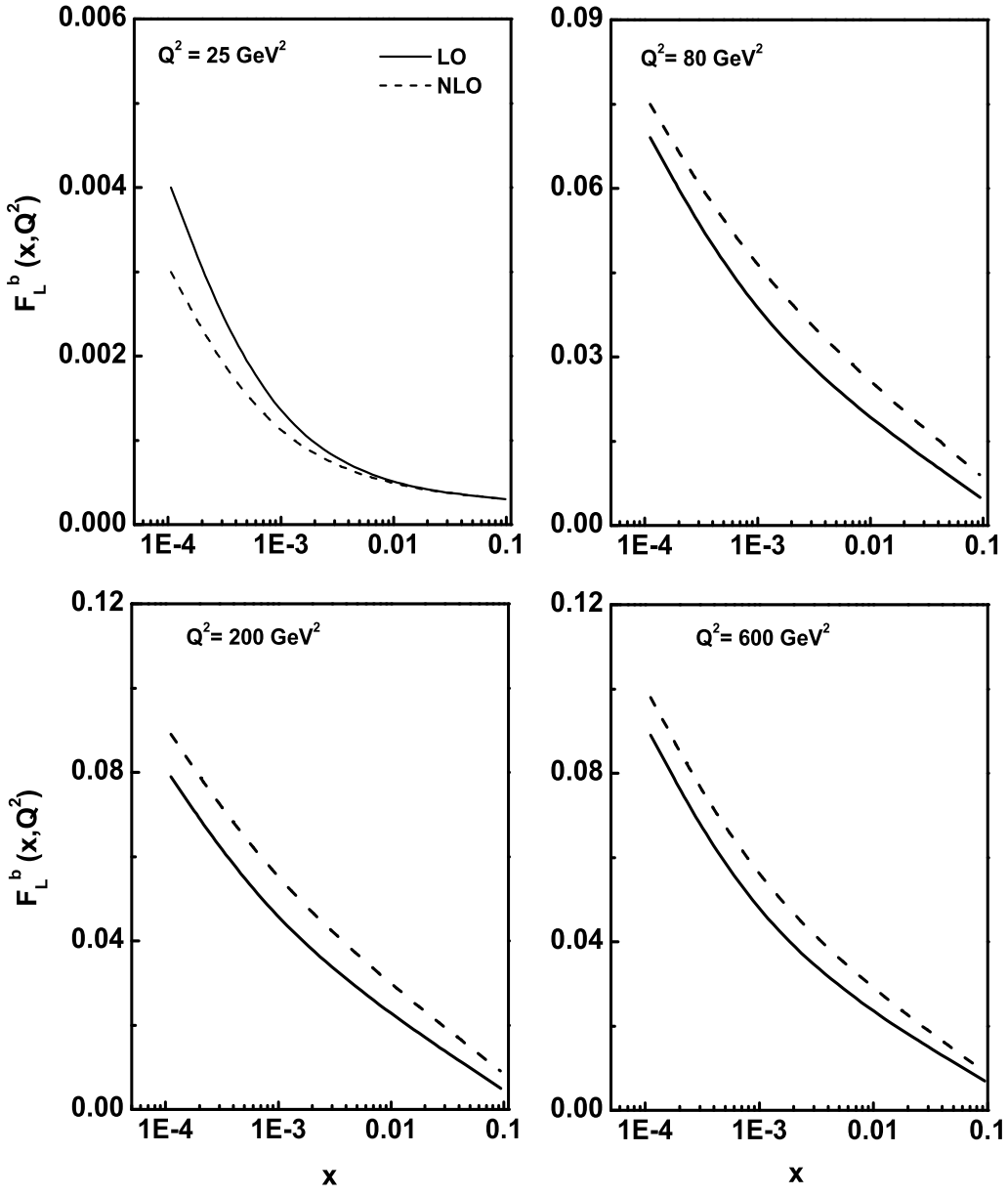

Figure 6.21: x-evolution results of F_L^b structure function using Regge theory with the input gluon distribution from DL model.

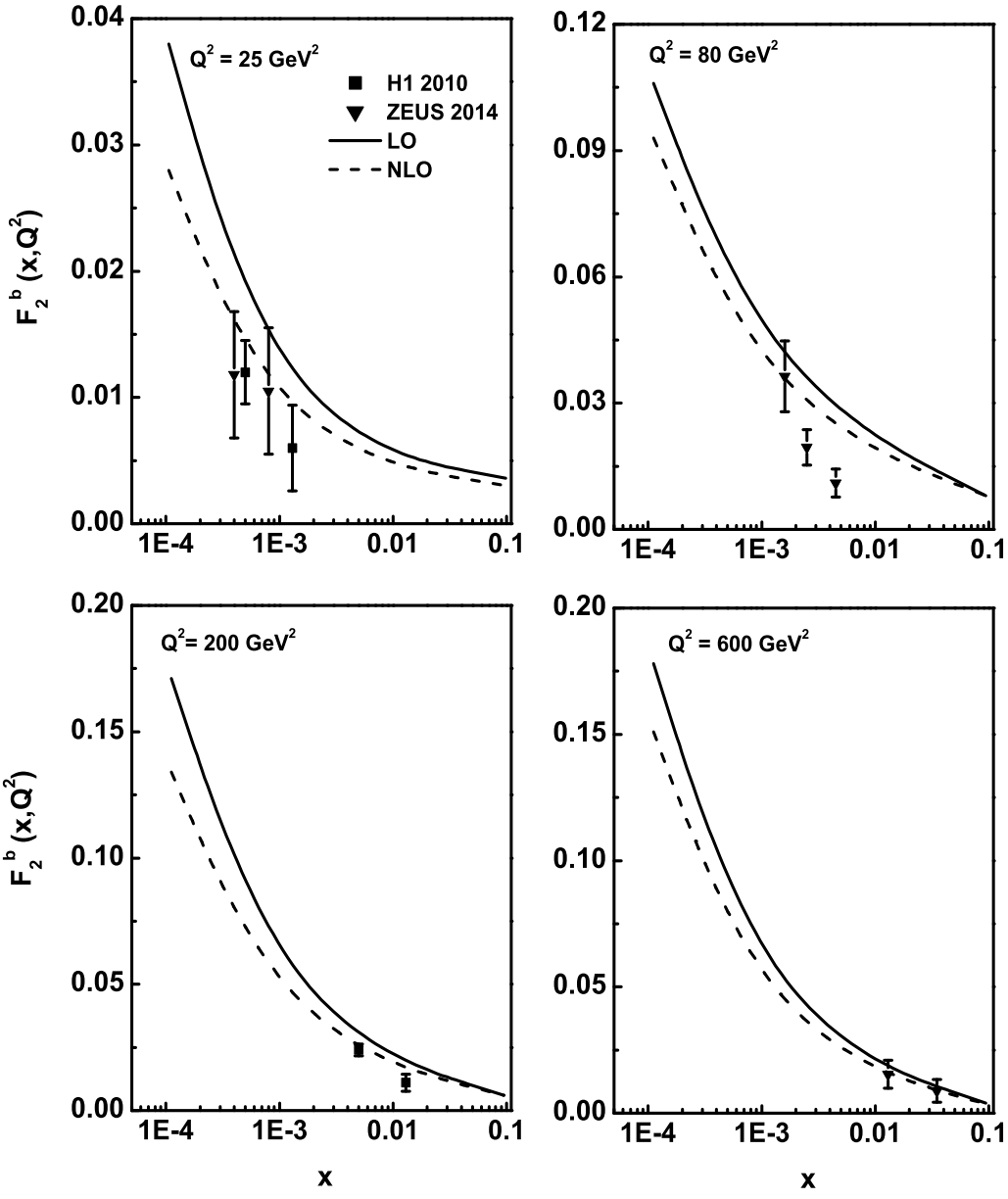

Figure 6.22: x-evolution results of F_2^b structure function using Regge theory in comparison with the H1, ZEUS data.

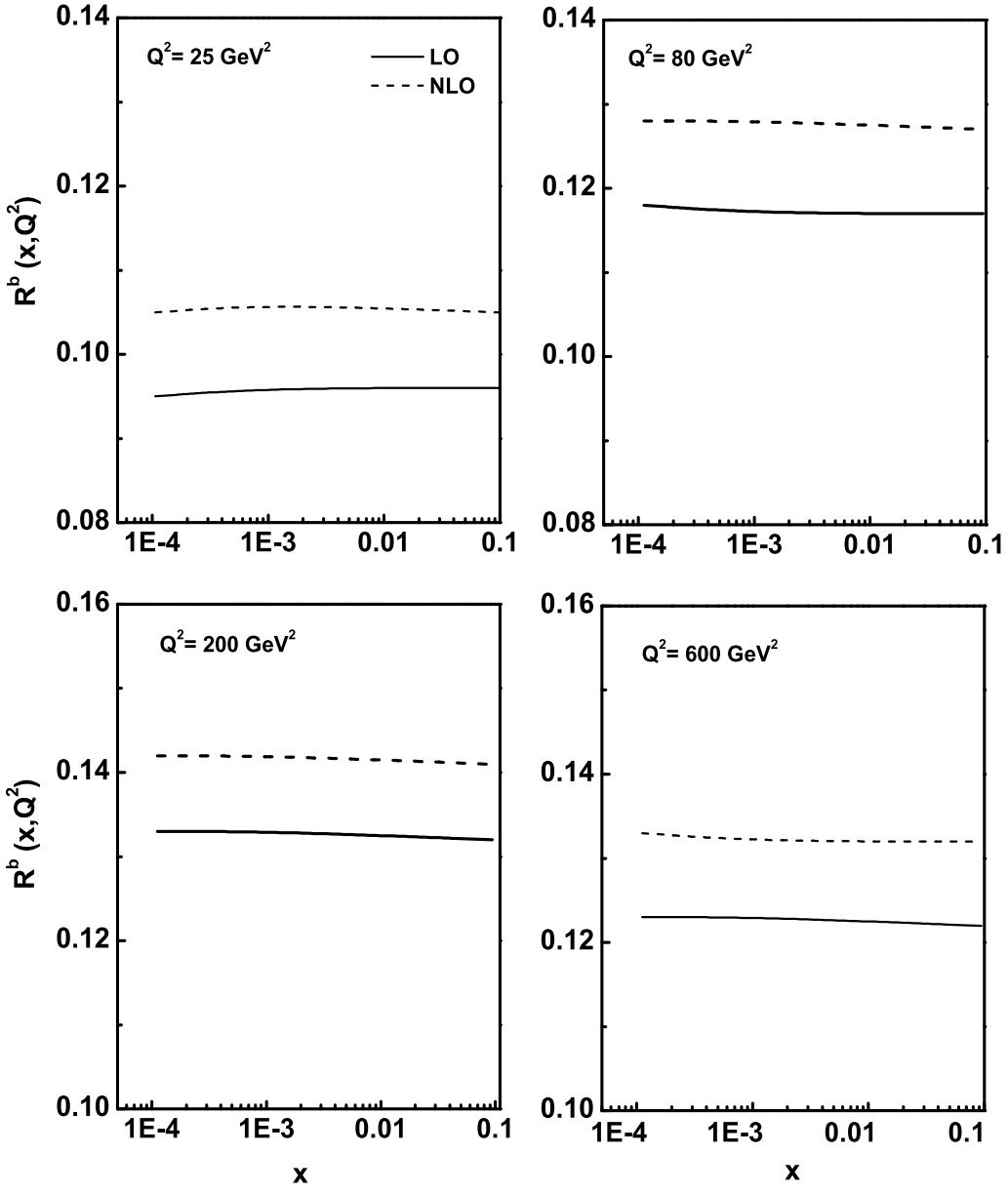

Figure 6.23: x-evolution results of the ratio of the beauty quark structure functions R^b using Regge theory.

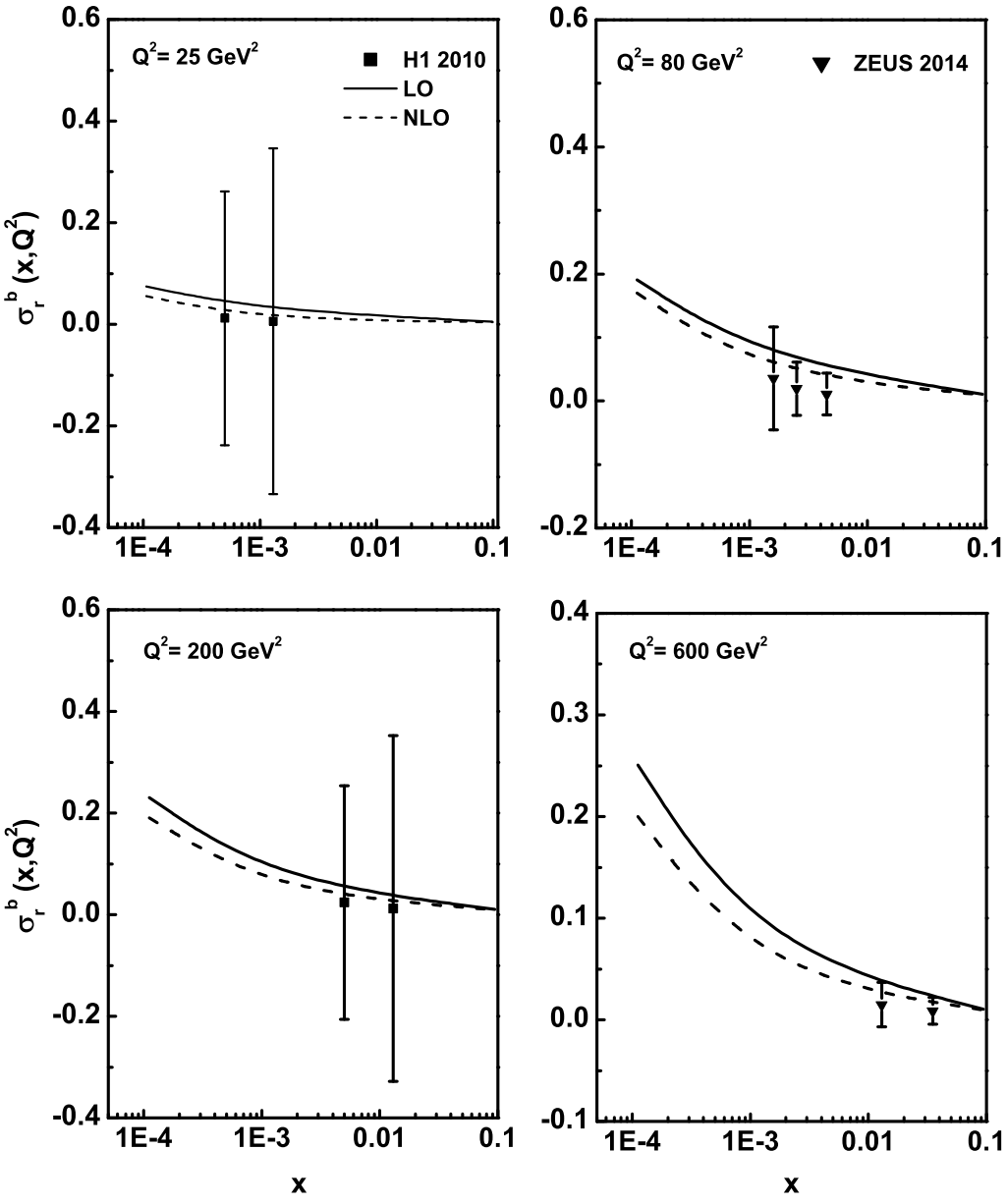

Figure 6.24: x-evolution results of the beauty quark reduced cross section σ_r^b using Regge theory in comparison with the H1, ZEUS data.

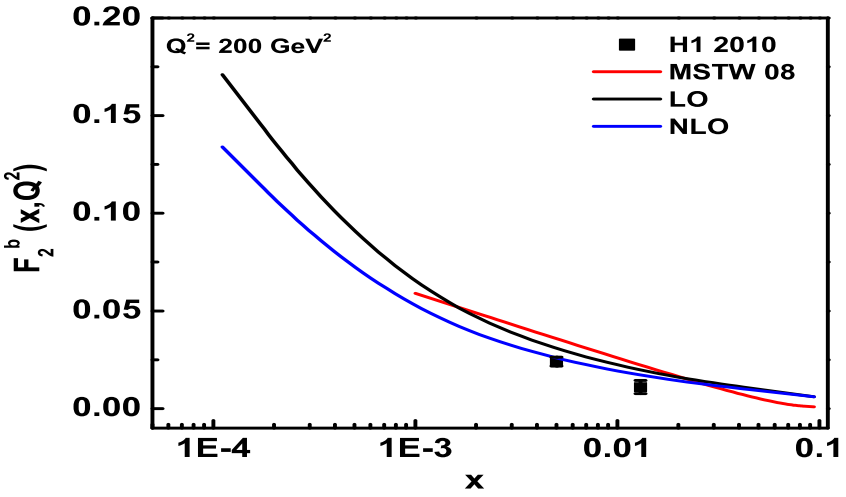

Figure 6.25: Comparison of our results of F_2^b at $Q^2 = 200GeV^2$ using Regge theory with the results of MSTW08 parameterization.

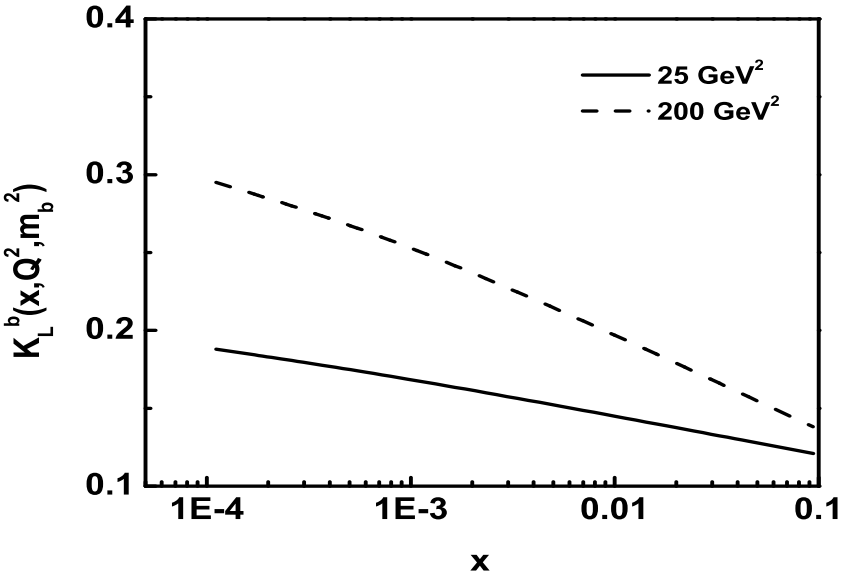

Figure 6.26: Results of the beauty content of F_L structure function K_L^b with respect to x at $Q^2 = 25, 200GeV^2$ using Regge theory.

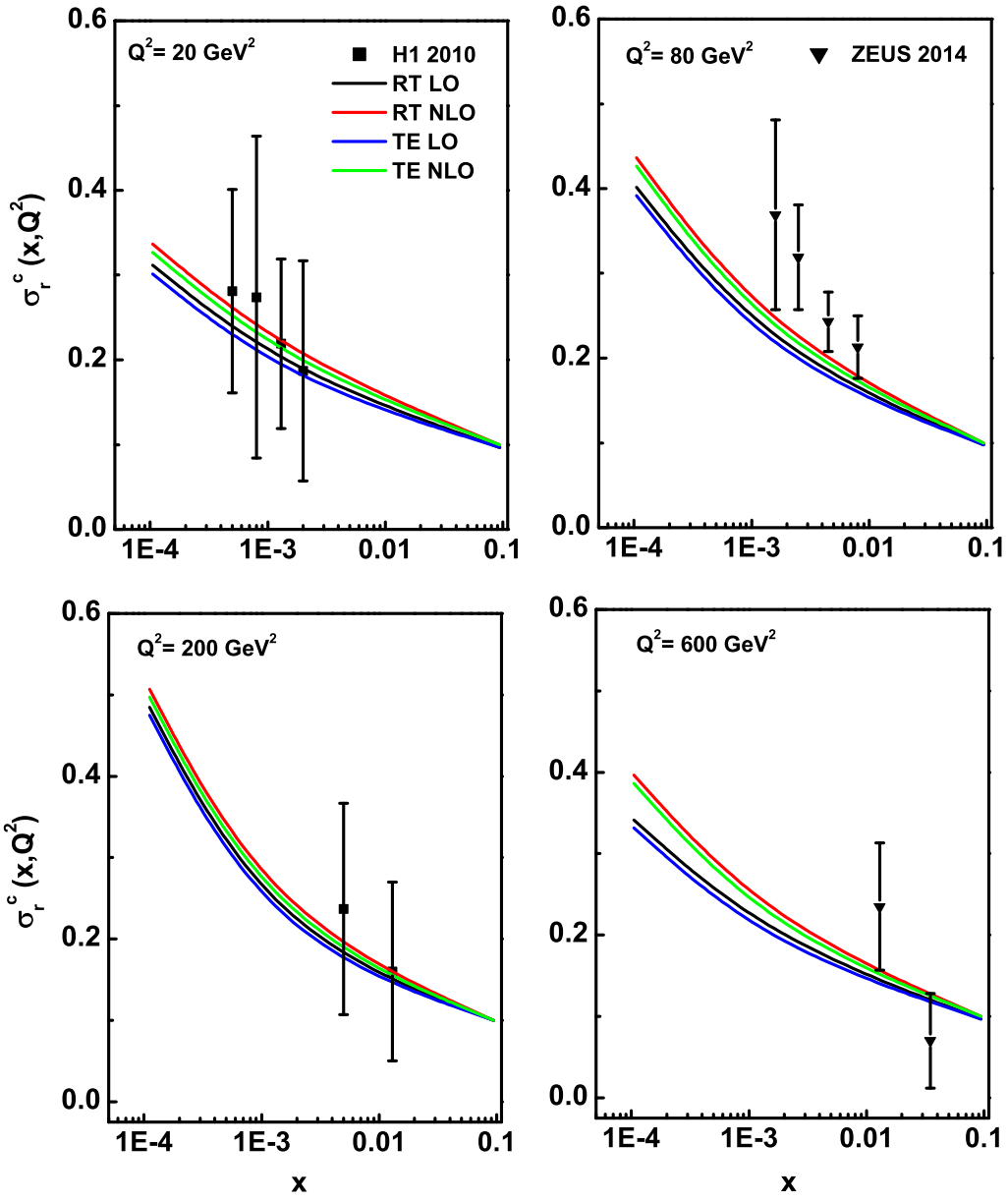

Figure 6.27: Comparison of our results of σ_r^c obtained by Taylor expansion (TE) method and Regge theory (RT).

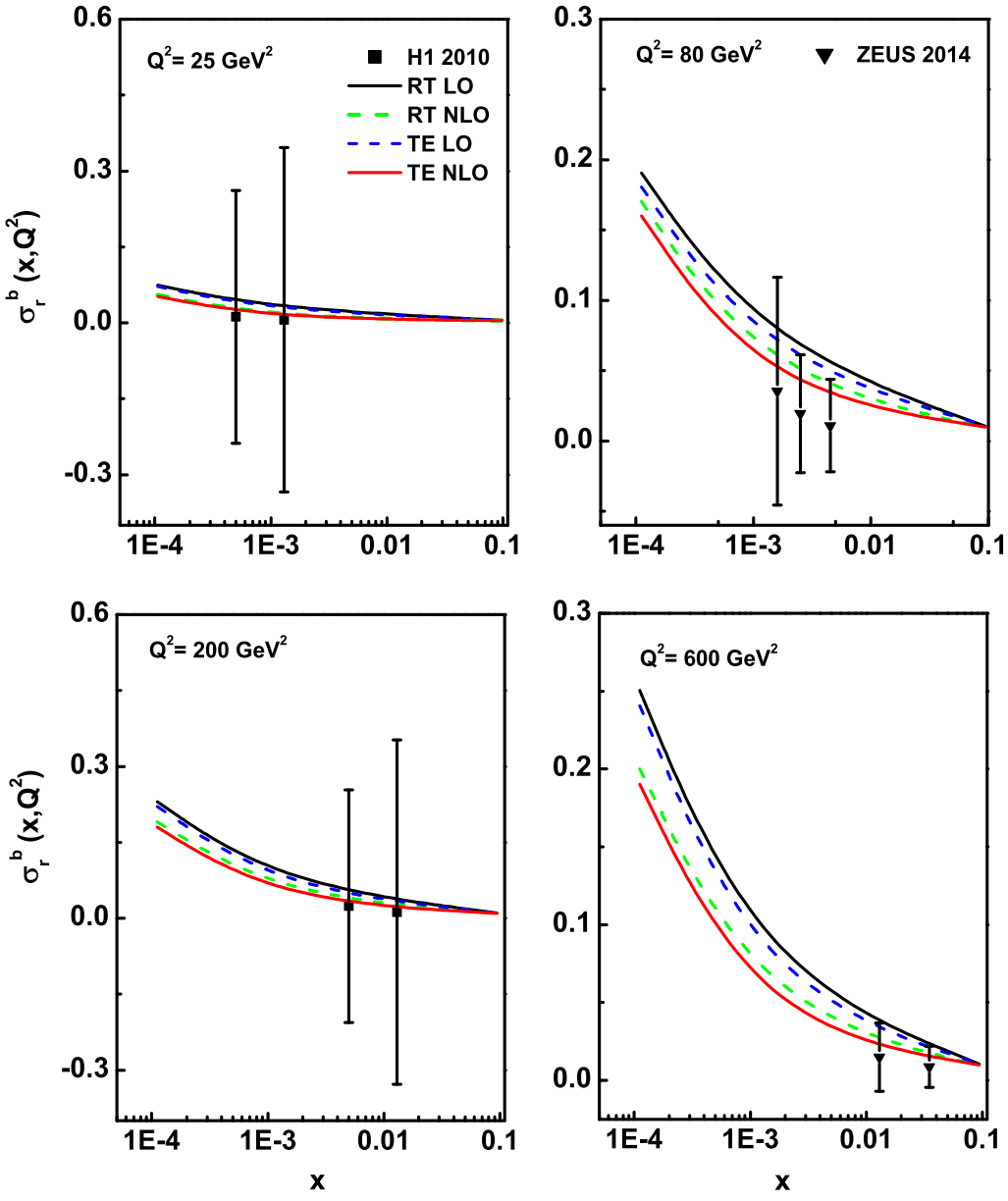

Figure 6.28: Comparison of our results of σ_r^b obtained by Taylor expansion (TE) method and Regge theory (RT).

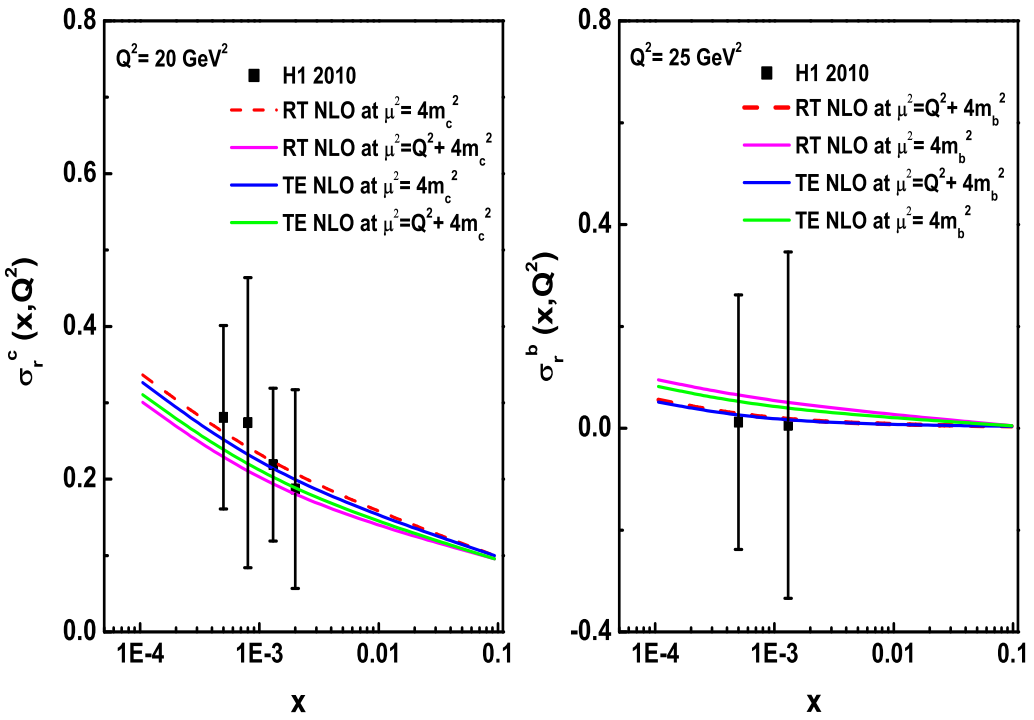

Figure 6.29: Sensitivity of our results of σ_r^b and σ_r^c with mass renormalization scale μ obtained by Taylor expansion (TE) method and Regge theory (RT).

renormalization scale μ obtained by both the methods i.e., Taylor expansion method and Regge theory method. This figure indicates that the sensitivity of our results with mass renormalization scale $\mu^2 = 4m_h^2 + Q^2$, shows good agreement with the experimental data. From the figure it is observed that the sensitivity of the choice of scale μ is relatively large in case of the small-x region than that of the high x region as in the small-x region the production of heavy quark is large compared to that in the high x region. In figure 6.29, in both the plots the behaviour of σ_r^c and σ_r^b with respect to x shows increasing behaviour towards small values of x. But in case of the charm quark the increase of the cross section is more sharp than that of the cross section in case of beauty quark. The reason for this is that the density of heavy beauty quark is less than

that of the charm quark in the small-x region. So, the charm cross section increases more sharply with respect to x than that of the beauty quark cross section.

6.3 Conclusions

In this chapter, we have calculated the heavy quark structure functions $F_k^h(k = 2, L; h = c, b)$ using gluon distribution function in NLO analysis with the help of Taylor expansion (TE) method and the Reege (RT) like behaviour of the structure function. The obtained results are compared with the experimental H1, ZEUS data, results of DL, CD model and MSTW08 parameterization which reflect compatibility of our results with the data and model fits. All the gluon dominating heavy quark structure functions show increasing behaviour towards small values of x. To confirm the validity of our calculations we have also analysed the behaviour of heavy quark structure function ratio R^h and reduced heavy quark cross section σ_r^h with respect to x which also shows good agreement with experimental data. We have also analysed the behaviour of heavy quark content of the longitudinal structure function with respect to x which reflects increasing behaviour towards small-x and high Q^2 region. In our calculations we have considered the value of the mass renormalization scale μ as $\mu^2 = 4m_h^2 + Q^2$. The sensitivity of our results of charm and beauty quark structure function with mass renormalization scale μ shows that at $\mu^2 = 4m_h^2 + Q^2$, our predicted results are compatible with the experimental data. Our predicted results in both the methods show good agreement with the experimental data, model fits and parameterization. Thus we can conclude that both the methods can be used to study the behaviour of the heavy quark structure functions.

References

[1] Carvalho, F., et al. Charm and longitudinal structure functions within the Kharzeev-Levin-Nardi model, *Phys. Rev. C* **79** (3), 035211-1–6, 2009.

[2] Donnachie, A. and Landshoff, P. V. The protons gluon distribution, *Phys. Lett. B* **550** (3-4), 160–165, 2002.

[3] Aaron, F. D., et al. Measurement of the charm and beauty structure functions using the H1 vertex detector at HERA, *Eur. Phys. J. C* **65** (1-2), 89–109, 2010.

[4] Abramowicz, H., et al. Measurement of beauty and charm production in deep inelastic scattering at HERA and measurement of the beauty-quark mass, *J. High Energy Phy.* **2014** (09), 127-1–55, 2014.

[5] Nikolaev, N. N. and Zoller, V. R. How open charm production and scaling violations probe the rightmost hard BFKL pole exchange, *Phys. Lett. B* **509** (3-4), 283–293 2001.

[6] Martin, A. D., et al. Parton distributions for the LHC, *Eur. Phys. J. C* **63** (2), 189–285, 2009.

[7] Gluck, M., Reya, E. and Vogt, A. Dynamical parton distributions of the proton and small x physics, *Z. Phys. C* **67** (3), 433–447, 1995.

[8] Gluck, M., Reya, E. and Vogt, A. Dynamical parton distributions revisited, *Eur. Phys. J. C* **5** (3), 461–470, 1998.

[9] Catani, S., Ciafaloni, M. and Hautmann, F. High energy factorization and small-x heavy flavour production, *Nucl. Phys. B* **366** (1), 135–188, 1991.

[10] Illarionov, A. Y., Kniehl, B. A. and Kotikov, A. V. Heavy-quark contributions to the ratio F_L/F_2 at low x, *Phys. Lett. B* **663** (1-2), 66–72, 2008.

[11] Baishya, R. and Sarma, J. K. Semi numerical solution of non-singlet Dokshitzer-GribovLipatovAltarelliParisi evolution equation up to next-to-next-to-leading order at small x, *Eur. Phys. J. C* **60** (4), 585–591, 2009.

[12] Laenen, E., et al. Complete $O(\alpha_S)$ corrections to heavy-flavour structure functions in electroproduction, *Nucl. Phys. B* **392** (1), 162–228, 1993.

[13] Kotikov, A. V. and Parente, G. The gluon distribution as a function of F_2 and $dF_2/dlnQ^2$ at small x. The next-to-leading analysis, *Phys. Lett. B* **379** (1-4), 195–201, 1996.

[14] Boroun, G. R. and Rezaei, B. NLO corrections to the hard pomeron behavior of the charm structure functions $F_k^c(k = 2, L)$ at low x, *Nucl. Phys. B* **857** (2), 143-152, 2012. □